Research Article

EASL EUROPEAN ASSOCIATION FOR THE STUDY OF THE LIVER | JOURNAL OF HEPATOLOGY

Common variation of IL28 affects gamma-GTP levels and inflammation of the liver in chronically infected hepatitis C virus patients

Hiromi Abe[1,2,3], Hidenori Ochi[1,2,3], Toshiro Maekawa[1,2], C. Nelson Hayes[1,2,3], Masataka Tsuge[3,4], Daiki Miki[1,2,3], Fukiko Mitsui[1,2,3], Nobuhiko Hiraga[1,2,3], Michio Imamura[1,2,3], Shoichi Takahashi[1,2,3], Waka Ohishi[3,5], Koji Arihiro[6], Michiaki Kubo[7], Yusuke Nakamura[7,8], Kazuaki Chayama[1,2,3,*]

[1]*Laboratory for Digestive Diseases, Center for Genomic Medicine, RIKEN, Hiroshima, Japan;* [2]*Department of Medicine and Molecular Science, Division of Frontier Medical Science, Programs for Biomedical Research, Graduate School of Biomedical Sciences, Hiroshima University, Hiroshima, Japan;* [3]*Liver Research Project Center, Hiroshima University, Hiroshima, Japan;* [4]*Natural Science Center for Basic Research and Development, Hiroshima University, Hiroshima, Japan;* [5]*Department of Clinical Studies, Radiation Effects Research Foundation, Hiroshima, Japan;* [6]*Department of Pathology, Hiroshima University Hospital, Hiroshima, Japan;* [7]*Laboratory for Genotyping Development, RIKEN Center for Genomic Medicine, Yokohama, Japan;* [8]*Laboratory of Molecular Medicine, Human Genome Center, The Institute of Medical Science, University of Tokyo, Tokyo, Japan*

Background & Aims: A common genetic variation at the IL28 locus has been found to affect the response of peg-interferon and ribavirin combination therapy against chronic hepatitis C virus (HCV) infection. An allele associated with a favorable response (rs8099917 T), which is the major allele in the majority of Asian, American, and European populations, has also been found to be associated with spontaneous eradication of the virus.
Methods: As no studies have yet analyzed the effect of the polymorphism on biochemical and inflammatory changes in chronic infection, we analyzed a cohort of patients with chronic hepatitis C ($n = 364$) for the effect of the IL28 polymorphism on viral, biochemical, and histological findings.
Results: We found that the proportion of HCV wild type core amino acids 70 and 91 was significantly greater ($p = 1.21 \times 10^{-4}$ and 0.034) and levels of gamma-GTP significantly lower ($p = 0.001$) in patients homozygous for the IL28 major allele. We also found that inflammation activity and fibrosis of the liver were significantly more severe in patients homozygous for the IL28 major allele ($p = 0.025$ and 0.036, respectively). Although the higher gamma-GTP levels were also associated with higher inflammatory activity and fibrosis, multivariate analysis showed that only the IL28 allele polymorphism, sex, alcohol consumption, and liver fibrosis were independently associated with gamma-GTP levels ($p = 0.001$, 0.0003, 0.0013, and 0.0348, respectively).
Conclusions: These results suggest that different cytokine profiles induced by the IL28 polymorphism resulted in different biochemical and inflammatory conditions during chronic HCV infection and contribute to the progression of liver diseases.

Keywords: IL28; SNP; Histological activity; Inflammation; gamma-GTP.
Received 23 November 2009; received in revised form 9 March 2010; accepted 29 March 2010; available online 31 May 2010
* Corresponding author at: Department of Medical and Molecular Science, Division of Frontier Medical Science, Programs for Biomedical Research, Graduate school of Biomedical Science, Hiroshima University, 1-2-3 Kasumi, Minami-ku, Hiroshima 734-8551, Japan. Tel.: +81 82 257 5190; fax: +81 82 255 6220.
E-mail address: chayama@hiroshima-u.ac.jp (K. Chayama).
Abbreviations: HCV, hepatitis C virus; SNP, single nucleotide polymorphism; ISDR, interferon sensitivity determining region; BMI, body mass index.

Introduction

Hepatitis C virus infection is one of the major causative agents of chronic hepatitis, liver cirrhosis, and hepatocellular carcinoma [1]. The best current therapeutic regimen is pegylated interferon and ribavirin combination therapy [2,3]. Although the eradication rate of the virus has been improved by extending the treatment period from the standard 48 to 72 weeks for genotype 1b infected patients, active viral replication still remains in nearly half of these patients [4].

Recent studies have identified both host and viral factors predictive of interferon therapy. Among the viral factors, a forty amino acid stretch in the NS5 region has been found to be predictive of response to interferon monotherapy [5,6]. More recently, Akuta et al. identified amino acid substitutions in the core region (core aa70 and 91) that are predictive for the effect of interferon and ribavirin combination therapy [7,8].

Among the host factors, many common polymorphisms in the human genome, including single nucleotide polymorphisms (SNP), have been identified [9–13]. We recently reported that a SNP in the MAPKAPK3 gene is associated with response to interferon therapy [14]. More recently, three groups of researchers found that several SNPs in the IL28 locus are related to the effectiveness of combination therapy [15–17]. We also performed a genome wide association study and confirmed that variation at the IL28 locus is related to the effectiveness of combination therapy (Chayama K, personal communication).

Research Article

These viral and host factors must influence the natural course of viral infection. Host immune cells produce interferon and other cytokines in response to viral infection. For RNA viruses such as HCV, cellular sensors such as RIG-I detect the double stranded RNA and activate a pathway to produce cytokines, including alpha and beta interferons that trigger an antiviral response to eradicate the virus [18]. Genetic polymorphism of genes involved in innate immunity is likely to influence the strength and nature of this defense. In fact, a polymorphism in the IL28 locus has been reported to correlate with spontaneous eradication of HCV [19]. However, little is known about how these factors affect the course of chronic infection of the virus. In this study, we focused on histological findings in the liver. We also analyzed viral and biochemical factors in patients chronically infected with HCV. We found that histological aspects of the liver (fibrosis and activity), HCV core amino acid substitutions, and gamma-GTP are associated with the polymorphism.

Materials and methods

Study subjects

We analyzed a cohort of 364 consecutive adult patients with chronic hepatitis C virus infection who visited Hiroshima University hospital and received liver biopsies between December 2002 and November 2008 and who agreed to provide blood samples for the human genome study. All patients included in the study had positive HCV viremia in serum for more than six months, assessed using a commercial quantitative polymerase chain reaction (PCR) assay (COBAS Amplicor HCV Monitor Test, v2.0; Roche Diagnostics, Branchburg, NJ). Patients with decompensated liver disease were excluded, as were patients co-infected with hepatitis B virus, or human immunodeficiency virus and patients with apparent auto-immune hepatitis and alcoholic liver disease. All patients provided written informed consent for the genomic analysis. The study protocol conforms to the ethical guidelines of the 1975 Declaration of Helsinki and was approved *a priori* by the ethical committees of Hiroshima University and Riken. The patient profiles are listed in Table 1. Using criteria reported by Desmet et al. [20], liver biopsy samples were evaluated by two pathologists. To verify consistency and accuracy, one of the pathologists independently re-evaluated samples analyzed by the other, and both pathologists were blind with respect to the IL28 polymorphism. We excluded insufficient or inconclusive biopsy samples, including those that were less than 10 mm^2 in size and containing less than 10 portal tracts. The amount of alcohol consumed was calculated according to the frequency of consumption and the alcohol concentration of beverages consumed. We estimated alcohol concentrations as follows: 5% for beer, 17% for sake, 25% for Japanese vodka, and 43% for whiskey; 1 ml of alcohol was considered equivalent to 0.886 g. The amount of alcohol consumed was divided into three categories: none, light (0–20 g/day), moderate (21–50 g/day). Heavy drinkers (more than 50 g/day) were excluded from the study.

Table 1. Characteristics of patients.

Characteristics of patients	
Age [median (range)]	59 (20–82)
Sex (male/female)	212/152
BMI [median (range)]	23 (16–39)
Alcohol consumption (Unavailable/none/0–20 g/day/21–50 g/day)	64/110/65/125
Hb [median (range)] mg/dl	14 (8–18)
Platelet [median(range)] × $10^4/mm^3$	14 (4–41)
ALT [median (range)]IU/L	62 (2–611)[c]
gamma-GTP [median (range)] IU/L	50 (7–680)
Genotype (1b/2a or 2b/1b + 2b/undertermined)	260/84/1/19
Fibrosis (F0/F1/F2/F3/F4)	4/116/141/66/37
Activity (A0/A1/A2/A3)	1/102/206/51
Virus titer [median (range)]kIU/l	1400 (<0.5–26,000)
Core 70[a] (wild/mutant/undertermined)	120/77/167
Core 91[a] (wild/mutant/undertermined)	107/88/169
ISDR[b] mutation (0/1/>2/undertermined)	58/70/48/188

[a] Hepatitis C virus core amino acid 70R and 91L are presented as wild type. Substituted amino acids are considered mutants.

[b] Interferon sensitivity determining region. Number of amino acids substituted from the prototype genotype 1b sequence were calculated.

[c] ALT levels of two patients remained around 2 IU/L even though AST and gamma-GTP levels were comparable to other chronic hepatitis C patients (peaking above 100 IU/L and returning to normal following SVR), probably due to deficiency of the ALT enzyme. These values were omitted from analysis of ALT.

Genotyping

Genotyping of some of the samples was performed as part of a genome wide association study using the Illumina HumanHap610-Quad Genotyping BeadChip (Illumina, Inc., CA) at Riken Yokohama Institute. Genotyping of the remaining samples was performed using TaqMan assay or Invader assay as described previously [21,22].

Analysis of amino acid sequences in the core and ISDR region

HCV RNA was extracted from 100 μl serum samples by SepaGene RV-R (Sanko Junyaku Co., Tokyo, Japan) and dissolved in 20 μl of H_2O. The RNA was then reverse transcribed with random primers and MMLV reverse transcriptase (Takara Shuzo, Tokyo, Japan). The resultant cDNA was then amplified by nested PCR. PCR was performed in 25 μl of reaction mixture containing 2.5 mM $MgCl_2$, 0.4 mM of each dNTP, 20 pmol of each primer and 1.25 U of LA Taq (Takara Bio Inc.) with a buffer supplied by the manufacturer. One microliter of 10×-diluted products from the first PCR was used as a template for the second PCR. The PCR primer sequences are listed in Table 2. The PCR protocol involved initial denaturation at 95 °C for 5 min, 35 cycles of denaturation for 30 s at 94 °C, annealing of primers for 1 min at 57 °C and extension for 1 min at 72 °C, followed by final extension at 72 °C for 7 min. The amplified DNA fragments were separated onto a 2% agarose gel and purified with the QIAquick gel extraction kit (Qiagen, Hilden, Germany). Nucleotide sequences were determined using the Big-Dye Terminator v3.1 Cycle Sequencing Kit (Applied Biosystems Inc., CA).The obtained nucleotide and amino acid sequences were compared with the prototype sequence of genotype 1b HCV-J (GenBank Accession Number D90208) [23]. Amino acids at positions 70 and 91 of the core region that were identical to the prototype (arginine and leucine, respectively) were considered wild type.

Statistical analysis

χ^2 and Mann–Whitney U-tests were applied to detect significant associations. Simple and multiple regression analyses were used to examine the association between serum gamma-GTP levels and the values of other markers. When the data were not normally distributed, Box-Cox power transformation was performed to remove skewness, followed by linear regression analyses. All of the statistical analyses were two sided, and $p < 0.05$ was considered significant. All statistical analysis was performed using the PASW Statistics 18 program (SPSS Inc., IL).

Results

IL28 locus genotypes and viral and biochemical markers

We compared viral and biochemical markers with IL28 genotypes. First we analyzed the relationship between IL28 genotypes

Table 2. Primers used in this study.

Core region	
Outer forward	5′-GCC ATA GTG GTC TGC GGA AC-3′
Outer reverse	5′-GGA GCA GTC CTT CGT GAC ATG-3′
Inner forward	5′-GCT AGC CGA GTA GTG TT-3′
Inner reverse	5′-GGA GCA GTC CTT CGT GAC ATG-3′
ISDR[a]	
Outer forward	5′-TTC CAC TAC GTG ACG GGC AT-3′
Outer reverse	5′-CCC GTC CAT GTG TAG GAC AT-3′
Inner forward	5′-GGG TCA CAG CTC CCA TGT GAG CC-3′
Inner reverse	5′-GAG GGT TGT AAT CCG GGC GTG C-3′

[a] Interferon sensitivity determining region.

Table 3. Amino acid substitutions in the core region of HCV and IL28 genotype.

SNP	Allele (1/2)	Genotype			p value[a]	OR
		11	12	22		(95% CI)[b]
rs8099917	T/G					
	Core aa70					
	Wild	2	17	101	1.21E-04	0.30
	Non-wild	3	28	46		(0.14–0.55)
	Core aa91					
	Wild	3	18	86	0.034	0.50
	Non-wild	2	27	59		(0.26–0.95)
	ISDR					
	0–1	2	37	89	0.120	1.90
	>2	2	7	39		(0.84–4.3)
	HCV genotype					
	1	6	63	190	0.443	0.81
	2	1	25	58		(0.47–1.4)

[a] p value by χ^2 test for the minor allele dominant model.
[b] Odds ratio for the minor allele in a dominant model.

Table 4. Factors associated with higher gamma-GTP levels.

Variable	Simple		Multiple	
	Estimate	p	Estimate	p
Age	−0.00004	0.899436		
Sex (male vs. female)	0.04647	5E-09	0.033	0.0003
BMI	−0.00257	0.044003		
Activity (A2–4 vs. A0–1)	−0.02518	0.004103	−0.015	0.1415
Fibrosis (F2–4 vs.F0–1)	−0.03	0.000382	−0.021	0.0348
Alcohol consumption	−0.03962	6.81E-06	−0.029	0.0013
IL28 genotype (2/2 vs. 1/2, 1/1)	0.02641	0.003522	0.03	0.001
HCV genotype (1 vs. 2)	−0.0068	0.471293		
Log virus titer (Log IU/ml)	0.00032	0.748826		
Core aa70 (wild vs. others)	−0.01589	0.117424		
Core aa91 (wild vs. others)	−0.01422	0.162341		
ISDR (0–1 vs. ⩾2)	0.00253	0.824685		

Simple and multiple regression analyses were used to examine the association between serum gamma-GTP and the values of other markers. All of the statistical analyses were two sided, and p <0.05 was considered significant.

and substitutions in the HCV core protein amino acids 70 and 91, as well as the HCV genotype and the number of amino acid substitutions in the ISDR. As shown in Table 3, there are significant associations between amino acid substitutions in the core region and the genotype of the rs8099917 SNP at the IL28B locus. In particular, patients homozygous for the major IL28 allele were significantly associated with wild type core amino acid 70 (OR = 0.30; p = 1.21E-04). A similar trend is seen with core amino acid 91 substitutions (OR = 0.50; p = 0.034). Patients with more than one amino acid substitution in the ISDR region also tended to occur in patients homozygous for the major allele, although the difference was not statistically significant (Table 3). There was no correlation between the HCV genotype and the IL28 allele.

We further examined the relationship between IL28 and biochemical markers such as ALT, gamma-GTP, total cholesterol, HDL cholesterol, serum iron, and HCV RNA levels. Only the gamma-GTP level was significantly associated with the IL28 genotype. As shown in Fig. 1A, the gamma-GTP levels were lowest in the IL28 major allele homozygotes and highest in minor allele homozygotes. As drinking alcohol is known to elevate gamma-GTP levels, we examined the effect of alcohol intake in our cohort. As shown in Fig. 1B, there was an association between alcohol and gamma-GTP levels. As we found that the gamma-GTP level is higher in patients with core amino acid 70 substitutions (Fig. 1C), we performed multivariate analysis to examine what factors contribute to higher levels of gamma-GTP. As shown in Table 4, a simple regression analysis revealed that serum gamma-GTP levels were associated with sex, BMI, inflammation activity, liver fibrosis, alcohol consumption, and IL28 genotype, whereas in multiple regression analysis, sex, liver fibrosis, alcohol consumption, and IL28 genotype remained positively associated with serum gamma-GTP levels.

Histological findings and polymorphism in the IL28 locus

We then analyzed the relationship between the IL28 locus polymorphisms and histological findings. We divided patients into mild fibrosis (F0 and F1) and severe fibrosis (F2–4) as well as lower activity (A0 and A1) and higher activity (A2 and A3) and compared these factors against IL28 genotypes. As shown in Table 5, both inflammatory activity and fibrosis were significantly associated with IL28 genotype. Inflammation was more active (A2–3) in patients homozygous for IL28 major alleles

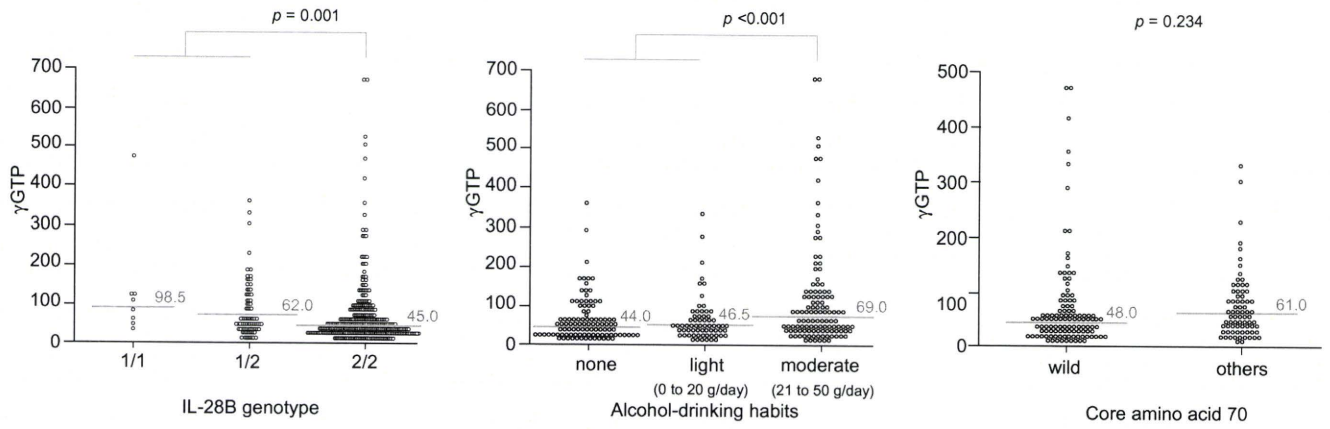

Fig. 1. gamma-GTP levels and IL28 genotype, alcohol intake, and core amino acid substitutions. gamma-GTP levels according to (A) IL28 genotypes, (B) alcohol consumption, and (C) core amino acid 70 substitutions are shown. Horizontal bars represent the median. Mann–Whitney U-test was used to compare gamma-GTP levels.

Research Article

Table 5. Histological findings and IL28 genotypes.

SNP	Allele (1/2)	Genotype			p value[a]	OR
		11	12	22		(95% CI)[b]
rs8099917	T/G					
	Fibrosis					
	F0–1	3	38	79	0.036	1.66
	F2–4	5	53	186		(1.03–2.69)
	Activity					
	A0–1	2	35	68	0.025	1.75
	A2–3	6	56	199		(1.07–2.86)

[a] p value by χ^2 test for the minor allele dominant model.
[b] Odds ratio for the minor allele in a dominant model.

(OR = 1.75; $p = 0.025$). Similarly, fibrosis was more severe in patients homozygous for IL28 major alleles (OR = 1.66; $p = 0.036$). We also performed analysis of the association of IL28 alleles and histological findings after adjusting for other factors that might influence the activity and fibrosis of the liver, such as age, gender, and alcoholic consumption. The IL28 allele was associated with F and A factors independently with adjustment for these predictive factors related to severity of liver fibrosis and inflammation (data not shown).

Relationship between histological activity, the IL28 allele, and gamma-GTP

As we described above, histological activity is more active in patients homozygous for IL28 major alleles. However, it seems contradictory that IL28 major allele homozygosity was associated with low levels of gamma-GTP, but severe activity was associated with high gamma-GTP. As shown in Fig. 2, however, when we compare the allele and activity the frequency of patients with higher activity (A2 and A3) were statistically more frequent in patients homozygous for major alleles (Fig. 2 and Table 5). When we compare gamma-GTP levels of A2 and A3 patients between patients homozygous for major alleles against the others, the levels were significantly lower in the major allele homozygous patients (Fig. 2). A0 and A1 patients showed similar results (Fig. 2). gamma-GTP levels are also significantly higher in patients with higher activities (A2 and A3) than in patients with lower activities (A0 and A1) (Fig. 2).

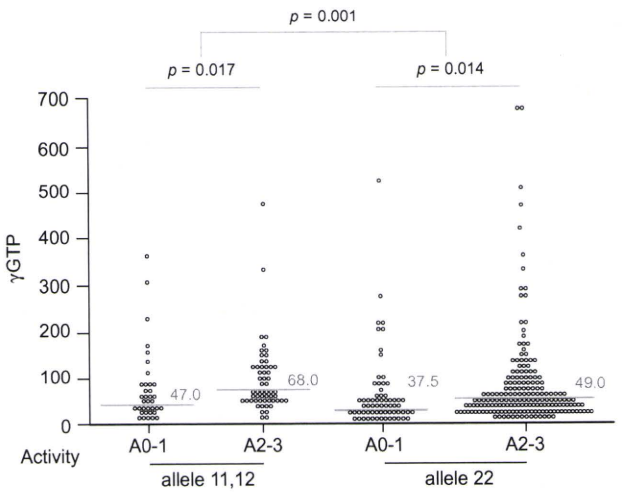

Fig. 2. Relationship between gamma-GTP levels, histological activity and IL28 genotype. gamma-GTP levels are plotted according to IL28 alleles, and histological activity. Horizontal bars represent the median. Mann–Whitney U-test was used to compare gamma-GTP levels.

Discussion

Polymorphism at the IL28 locus has been reported to be associated with the effectiveness of interferon and ribavirin combination therapy [15–17]. We have also found that the polymorphism is associated with the effect of interferon monotherapy on genotype 1b infected patients as well as genotype 2a infection in Japanese as well as Taiwanese patients (Chayama K, personal communication). The polymorphism has also been reported to be associated with spontaneous eradication of the hepatitis C virus [19]. As levels of IL28 gene transcripts have been reported to be higher in patients homozygous for the interferon response allele [16,17], we hypothesized that the polymorphism is also associated with inflammation and progression of chronic hepatitis. As expected, there were significant associations between IL28 genotypes and histological inflammatory activity as well as the degree of fibrosis in chronically HCV infected patients (Table 5). It seems reasonable that the inflammation is stronger in patients with elevated IL28 production because this molecule induces expression of interferon stimulated genes, including some inflammatory cytokines. As the polymorphism is associated with the effect of interferon therapy, the interferon therapy performed before biopsy might alter the results. In fact, a part of patients in this study were treated with peg-interferon and ribavirin combination therapy and the treatment outcome was associated with IL28 genotypes and core amino acid substitutions (data not shown). However, when we analyzed the relation between the IL28 allele and histological findings or core amino acid substitutions in only treatment-naïve patients, the results were unchanged, suggesting that the results obtained in this study are applicable without regard to history of interferon therapy.

Interestingly, the IL28 genotype was also associated with gamma-GTP levels and core amino acid substitutions, both of which are known to be predictive of response to interferon and ribavirin combination therapy [7,8,24]. The levels of liver enzymes such as ALT, AST, and gamma-GTP are usually higher in patients with high inflammatory activity. However, we observed that the levels were actually lower in patients with the favorable allele at the IL28 locus (the major allele in the Japanese population) (Figs. 1A and 2). A lower level of gamma-GTP has been reported to be associated with positive response to combination therapy. Further studies are needed to clarify the mechanism underlying the relation between gamma-GTP levels and therapy effectiveness. It would also be interesting to study the relationship between the IL28 allele and steatosis in the liver because gamma-GTP tends to be elevated in patients with steatosis, and steatosis caused by HCV core protein has been reported [25].

Similarly, viral wild type core amino acids 70 and 91 (i.e., core 70R and 91L), which were already known to be associated with positive response to combination therapy [7,8], were also found to be associated with the favorable human IL28 alleles (Table 3). If viruses with wild type core amino acids 70 and 91 are more

susceptible to interferon therapy, such strains should be less frequent in patients with higher cytokine levels. Viruses with wild type core 70 and 91 amino acids must therefore have some survival advantage in order to replicate in cells in which the level of IL28 production is high. Searching for a target molecule in the signaling cascade from sensing of the virus to production of IL28 might help resolve this question.

We also observed an association between high gamma-GTP levels and core amino acid 70 and 91 substitutions (Fig. 1C), although in multivariate analysis only IL28 genotype, liver fibrosis, sex, and alcohol consumption were significant predictors of gamma-GTP. It seems likely that these factors mutually interact in the presence of the virus and cytokines. Understanding these relationships will reveal the mechanism underlying the effective response to combination therapy and may suggest new strategies to cope with the hepatitis C virus.

Financial disclosure

The authors who have taken part in this study declare that they do not have anything to disclose regarding funding or conflict of interest with respect to this manuscript.

Acknowledgments

The authors thank Rie Akiyama, Yoshie Yoshida, Kazuyo Hattori, Mariko Shiota, Hiromi Ishino, Yasufumi Hayashida, and Takako Yokogi for excellent technical assistance, and Junko Sakamiya, Aya Furukawa, Mika Tsuzuno, Sakura Akamatus, Sanae Furuya, and other secretary members for their secretarial assistance. Part of this work was carried out at the Analysis Center of Life Science, Hiroshima University. This work was supported in part by Grants-in-Aid for scientific research and development from the Ministry of Health, Labor, and Welfare and Ministry of Education Culture Sports Science and Technology, Government of Japan.

References

[1] Barrera JM, Bruguera M, Ercilla MG, Gil C, Celis R, Gil MP, et al. Persistent hepatitis C viremia after acute self-limiting posttransfusion hepatitis C. Hepatology 1995;21:639–644.
[2] Hadziyannis SJ, Sette Jr H, Morgan TR, Balan V, Diago M, Marcellin P, et al. Peginterferon-alpha2a and ribavirin combination therapy in chronic hepatitis C: a randomized study of treatment duration and ribavirin dose. Ann Intern Med 2004;140:346–355.
[3] Manns MP, McHutchison JG, Gordon SC, Rustgi VK, Shiffman M, Reindollar R, et al. Peginterferon alfa-2b plus ribavirin compared with interferon alfa-2b plus ribavirin for initial treatment of chronic hepatitis C: a randomised trial. Lancet 2001;358:958–965.
[4] Jensen DM, Marcellin P, Freilich B, Andreone P, Di Bisceglie A, Brandao-Mello CE, et al. Re-treatment of patients with chronic hepatitis C who do not respond to peginterferon-alpha2b: a randomized trial. Ann Intern Med 2009;150:528–540.
[5] Enomoto N, Sakuma I, Asahina Y, Kurosaki M, Murakami T, Yamamoto C, et al. Mutations in the nonstructural protein 5A gene and response to interferon in patients with chronic hepatitis C virus 1b infection. N Engl J Med 1996;334:77–81.
[6] Enomoto N, Sakuma I, Asahina Y, Kurosaki M, Murakami T, Yamamoto C, et al. Comparison of full-length sequences of interferon-sensitive and resistant hepatitis C virus 1b. Sensitivity to interferon is conferred by amino acid substitutions in the NS5A region. J Clin Invest 1995;96:224–230.
[7] Akuta N, Suzuki F, Kawamura Y, Yatsuji H, Sezaki H, Suzuki Y, et al. Predictive factors of early and sustained responses to peginterferon plus ribavirin combination therapy in Japanese patients infected with hepatitis C virus genotype 1b: amino acid substitutions in the core region and low-density lipoprotein cholesterol levels. J Hepatol 2007;46:403–410.
[8] Akuta N, Suzuki F, Sezaki H, Suzuki Y, Hosaka T, Someya T, et al. Predictive factors of virological non-response to interferon-ribavirin combination therapy for patients infected with hepatitis C virus of genotype 1b and high viral load. J Med Virol 2006;78:83–90.
[9] Welzel TM, Morgan TR, Bonkovsky HL, Naishadham D, Pfeiffer RM, Wright EC, et al. Variants in interferon-alpha pathway genes and response to pegylated interferon-Alpha2a plus ribavirin for treatment of chronic hepatitis C virus infection in the hepatitis C antiviral long-term treatment against cirrhosis trial. Hepatology 2009;49:1847–1858.
[10] Hijikata M, Ohta Y, Mishiro S. Identification of a single nucleotide polymorphism in the MxA gene promoter (G/T at nt −88) correlated with the response of hepatitis C patients to interferon. Intervirology 2000;43:124–127.
[11] Knapp S, Yee LJ, Frodsham AJ, Hennig BJ, Hellier S, Zhang L, et al. Polymorphisms in interferon-induced genes and the outcome of hepatitis C virus infection: roles of MxA, OAS-1 and PKR. Genes Immun 2003;4:411–419.
[12] Matsuyama N, Mishiro S, Sugimoto M, Furuichi Y, Hashimoto M, Hijikata M, et al. The dinucleotide microsatellite polymorphism of the IFNAR1 gene promoter correlates with responsiveness of hepatitis C patients to interferon. Hepatol Res 2003;25:221–225.
[13] Naito M, Matsui A, Inao M, Nagoshi S, Nagano M, Ito N, et al. SNPs in the promoter region of the osteopontin gene as a marker predicting the efficacy of interferon-based therapies in patients with chronic hepatitis C. J Gastroenterol 2005;40:381–388.
[14] Tsukada H, Ochi H, Maekawa T, Abe H, Fujimoto Y, Tsuge M, et al. A polymorphism in MAPKAPK3 affects response to interferon therapy for chronic hepatitis C. Gastroenterology 2009;136:1796–1805, e1796.
[15] Ge D, Fellay J, Thompson AJ, Simon JS, Shianna KV, Urban TJ, et al. Genetic variation in IL28B predicts hepatitis C treatment-induced viral clearance. Nature 2009;461:399–401.
[16] Suppiah V, Moldovan M, Ahlenstiel G, Berg T, Weltman M, Abate ML, et al. IL28B is associated with response to chronic hepatitis C interferon-alpha and ribavirin therapy. Nat Genet 2009;41:1100–1104.
[17] Tanaka Y, Nishida N, Sugiyama M, Kurosaki M, Matsuura K, Sakamoto N, et al. Genome-wide association of IL28B with response to pegylated interferon-alpha and ribavirin therapy for chronic hepatitis C. Nat Genet 2009;41:1105–1109.
[18] Yoneyama M, Kikuchi M, Natsukawa T, Shinobu N, Imaizumi T, Miyagishi M, et al. The RNA helicase RIG-I has an essential function in double-stranded RNA-induced innate antiviral responses. Nat Immunol 2004;5:730–737.
[19] Thomas DL, Thio CL, Martin MP, Qi Y, Ge D, O'Huigin C, et al. Genetic variation in IL28B and spontaneous clearance of hepatitis C virus. Nature 2009;461:798–801.
[20] Desmet VJ, Gerber M, Hoofnagle JH, Manns M, Scheuer PJ. Classification of chronic hepatitis: diagnosis, grading and staging. Hepatology 1994;19:1513–1520.
[21] Ohnishi Y, Tanaka T, Ozaki K, Yamada R, Suzuki H, Nakamura Y. A high-throughput SNP typing system for genome-wide association studies. J Hum Genet 2001;46:471–477.
[22] Suzuki A, Yamada R, Chang X, Tokuhiro S, Sawada T, Suzuki M, et al. Functional haplotypes of PADI4, encoding citrullinating enzyme peptidylarginine deiminase 4, are associated with rheumatoid arthritis. Nat Genet 2003;34:395–402.
[23] Kato N, Hijikata M, Ootsuyama Y, Nakagawa M, Ohkoshi S, Sugimura T, et al. Molecular cloning of the human hepatitis C virus genome from Japanese patients with non-A, non-B hepatitis. Proc Natl Acad Sci USA 1990;87:9524–9528.
[24] Bergmann JF, Vrolijk JM, van der Schaar P, Vroom B, van Hoek B, van der Sluys Veer A, et al. Gamma-glutamyltransferase and rapid virological response as predictors of successful treatment with experimental or standard peginterferon-alpha-2b in chronic hepatitis C non-responders. Liver Int 2007;27:1217–1225.
[25] Moriya K, Fujie H, Shintani Y, Yotsuyanagi H, Tsutsumi T, Ishibashi K, et al. The core protein of hepatitis C virus induces hepatocellular carcinoma in transgenic mice. Nat Med 1998;4:1065–1067.

Journal of General Virology (2010), **91**, 1854–1864 DOI 10.1099/vir.0.019224-0

HBx protein is indispensable for development of viraemia in human hepatocyte chimeric mice

Masataka Tsuge,[1,2,3] Nobuhiko Hiraga,[1,3] Rie Akiyama,[1,3] Sachi Tanaka,[1,3] Miyuki Matsushita,[1,3] Fukiko Mitsui,[1,3] Hiromi Abe,[1,4] Shosuke Kitamura,[1,3] Tsuyoshi Hatakeyama,[1,3] Takashi Kimura,[1,3] Daiki Miki,[1,3] Nami Mori,[1,3] Michio Imamura,[1,3] Shoichi Takahashi,[1,3] C. Nelson Hayes[1,3] and Kazuaki Chayama[1,3,4]

Correspondence
Kazuaki Chayama
chayama@hiroshima-u.ac.jp

[1]Department of Medicine and Molecular Science, Division of Frontier Medical Science, Programs for Biomedical Research, Graduate School of Biomedical Sciences, Hiroshima University, Hiroshima, Japan

[2]Natural Science Center for Basic Research and Development, Hiroshima University, Hiroshima, Japan

[3]Liver Research Project Center, Hiroshima University, Hiroshima, Japan

[4]Laboratory for Liver Diseases, SNP Research Center, The Institute of Physical and Chemical Research (RIKEN), Yokohama, Japan

The non-structural X protein, HBx, of hepatitis B virus (HBV) is assumed to play an important role in HBV replication. Woodchuck hepatitis virus X protein is indispensable for virus replication, but the duck hepatitis B virus X protein is not. In this study, we investigated whether the HBx protein is indispensable for HBV replication *in vivo* using human hepatocyte chimeric mice. HBx-deficient (HBx-def) HBV was generated in HepG2 cells by transfection with an overlength HBV genome. Human hepatocyte chimeric mice were infected with HBx-def HBV with or without hepatic HBx expression by hydrodynamic injection of HBx expression plasmids. Serum virus levels and HBV sequences were determined with mice sera. The generated HBx-def HBV peaked in the sucrose density gradient at points equivalent to the generated HBV wild type and the virus in a patient's serum. HBx-def HBV-injected mice developed measurable viraemia only in continuously HBx-expressed liver. HBV DNA in the mouse serum increased up to 9 $\log_{10}$ copies ml^{-1} and the viraemia persisted for more than 2 months. Strikingly, all revertant viruses had nucleotide substitutions that enabled the virus to produce the HBx protein. It was concluded that the HBx protein is indispensable for HBV replication and could be a target for antiviral therapy.

Received 15 December 2009
Accepted 5 March 2010

INTRODUCTION

Chronic hepatitis B virus (HBV) infection is associated with the development of virus-related liver diseases, including chronic hepatitis, liver cirrhosis and hepatocellular carcinoma (HCC). HBV is a member of the family *Hepadnaviridae*, which consists of hepatotropic, small DNA viruses that infect their respective animal hosts (Ando *et al.*, 1999; Ganem & Schneider, 2001; Raney & McLachlan, 1991). HBV particles contain a 3.2 kb partially double-stranded circular DNA genome encoding four open reading frames (ORFs). The preS/S, pre-core/core, polymerase/reverse transcriptase and non-structural X protein (HBx) mRNAs are transcribed from each of the four ORFs (Seeger & Mason, 2000; Tang *et al.*, 2001). Although previous works have demonstrated that HBx protein is necessary for maximal HBV replication in cultured cells (Bouchard *et al.*, 2001; Keasler *et al.*, 2007; Leupin *et al.*, 2005; Tang *et al.*, 2005) and in mouse hepatocytes (Keasler *et al.*, 2007), the precise function of HBx in the virus life cycle remains poorly defined in human hepatocytes under physiological conditions because there is no natural infection–replication system available. Accordingly, all previous work has been done using hepatocarcinoma cell lines with transfection or mouse hepatocytes with hydrodynamic injection. Analysis of HBx under physiological conditions will provide more accurate information for the function of the HBx protein.

The nucleotide and amino acid sequences of the X genes are well-conserved among all mammalian hepadnaviruses. Expression of HBx protein in hepatocytes has been reported

The GenBank/EMBL/DDBJ accession number for the nucleotide sequence of the HBV genome cloned into plasmid pTRE-HB-wt is AB206817.

both in humans (Su *et al.*, 1998) and in woodchucks (Dandri *et al.*, 1996; Jacob *et al.*, 1997). Previous reports have shown that the X protein of the woodchuck hepatitis virus (WHV) is important for the virus life cycle (Chen *et al.*, 1993; Sitterlin *et al.*, 2000a; Zhang *et al.*, 2001; Zoulim *et al.*, 1994). In contrast, in non-oncogenic avian hepatitis viruses, such as duck hepatitis B virus (DHBV), the X protein (DHBx) is not necessary for virus replication *in vivo* (Meier *et al.*, 2003). The HBx and WHV X proteins (WHx) localize both in the cytoplasm and in the nucleus (Dandri *et al.*, 1998; Doria *et al.*, 1995; Sitterlin *et al.*, 2000b; Wang *et al.*, 1991), and both of them have similar multi-phasic activities for transcription, DNA repair, cell growth and apoptotic cell death in tissue-culture cells (Arbuthnot *et al.*, 2000; Murakami, 2001). HBx and WHx have also been shown to stimulate virus replication in cell lines by activating viral transcription (Colgrove *et al.*, 1989; Melegari *et al.*, 2005; Zhang *et al.*, 2001) or by enhancing the reverse transcription activity of the viral polymerase (Bouchard *et al.*, 2001; Klein *et al.*, 1999). Although it has been shown that the WHx protein is indispensable for virus replication *in vivo* (Zoulim *et al.*, 1994), which of the above functions is indispensable remains unknown. As HBV infects only humans and chimpanzees, it has been difficult to perform intensive studies *in vivo*.

Recently, Mercer *et al.* (2001) reported that transplanted human hepatocytes in SCID mice homozygous for the Alb-uPA transgene resulted in replacement of the mouse liver. They also reported that the highly replaced mice are susceptible to hepatitis C virus (Mercer *et al.*, 2001). Tateno *et al.* (2004) also created human hepatocyte chimeric mice with an improved replacement rate. Using this chimeric mouse model and the cell-culture-created HBV, we showed previously that hepatitis B e antigen (HBeAg) is dispensable for virus infection and replication (Tsuge *et al.*, 2005).

In this study, we tested whether the cell-culture-generated HBx-defective (HBx-def) HBV infects and replicates in the chimeric mice. As HBx-def HBV did not develop measurable viraemia, we expressed the HBx protein in the chimeric mouse liver by hydrodynamically injecting HBx-expression plasmid. It was noted that this *trans*-complementation of HBx helped the replication of HBx-def virus in the chimeric mice, and revertant viruses showed nucleotide substitutions that reversed the introduced stop codon [CAA to TAA created by a C-to-T point mutation at nt 1395 (aa 7) in the HBx gene; Fig. 1a] and restored expression. The HBx protein is thus indispensable for infection and proliferation of HBV. The protein thus might be a target for therapy development against HBV.

RESULTS

Production of HBV particles and antigens in cell culture and effect of HBx ablation

We initially examined nucleotide sequences of the cell-line-produced HBV by direct sequencing of the PCR products using cell-culture supernatants. As expected, HBV DNA was released from HepG2 cells transfected with the HBx-def plasmid with an introduced stop codon mutation by calcium phosphate precipitation (data not shown). We then analysed hepatitis B surface antigen (HBsAg), HBeAg and HBV DNA in the supernatants 3 days after transfection. While HBV DNA titres were not significantly different between the wild-type (WT)- and HBx-def HBV-transfected cultures, the HBsAg and the HBeAg levels were significantly lower in HBx-def HBV- than in WT-transfected cultures (Fig. 1b).

To examine the particle formation in the transfection experiments, we analysed the density of generated HBV by sucrose density gradient sedimentation analysis. The density of the cell-culture-produced HBx-def HBV was compared with those of WT HBV and HBV obtained from human serum. As shown in Fig. 1(c), each of the three preparations of HBV sedimented at sucrose density 1.18 g ml^{-1}, suggesting that cell-culture-produced HBV particles were similar to those obtained from human serum.

Infectivity of HBx-def HBV particles

To analyse the infectivity of HBx-def HBV, we inoculated cell-culture-produced recombinant HBV (WT HBV or HBx-def HBV) into chimeric mice. All seven mice injected with cell-culture-generated WT HBV developed measurable viraemia 2–7 weeks after inoculation. The virus titre reached 6–10 log_{10} copies ml^{-1} and the viraemia persisted for more than 4 months (Fig. 2a). In contrast, we did not observe any measurable viraemia in HBx-def HBV-injected mice within a period of 16 weeks after inoculation (Fig. 2b). Only five of 16 HBx-def HBV-inoculated mice became occasionally positive for HBV DNA by nested PCR assay. We then examined the mouse livers 14 weeks after inoculation by immunohistochemical staining with anti-HB core (HBc) antibody. As shown in Fig. 2(c), human hepatocytes of WT-injected mice were positive for HBV core antigen (HBcAg). In contrast, the staining was negative in mouse liver injected with HBx-def HBV.

Effect of *trans*-complementation of entire and partial HBx protein on replication of HBx-def HBV

We then investigated the effect of *trans*-complementation of the HBx protein both *in vitro* and *in vivo*. Since the C-terminal two-thirds (aa 51–154) domain of HBx has been reported to contain a transactivation domain (Tang *et al.*, 2005), we constructed three plasmids (full length and residues 1–50 and 51–154), as shown in Fig. 3(a). To analyse the effect of co-transfection of these three plasmids on intracellular replication of HBV, the cells transfected using *Trans*IT-LT1 reagent were harvested 24 h after transfection and analysed by Southern blotting. As shown in Fig. 3(b), *trans*-complementation of HBx enhanced the

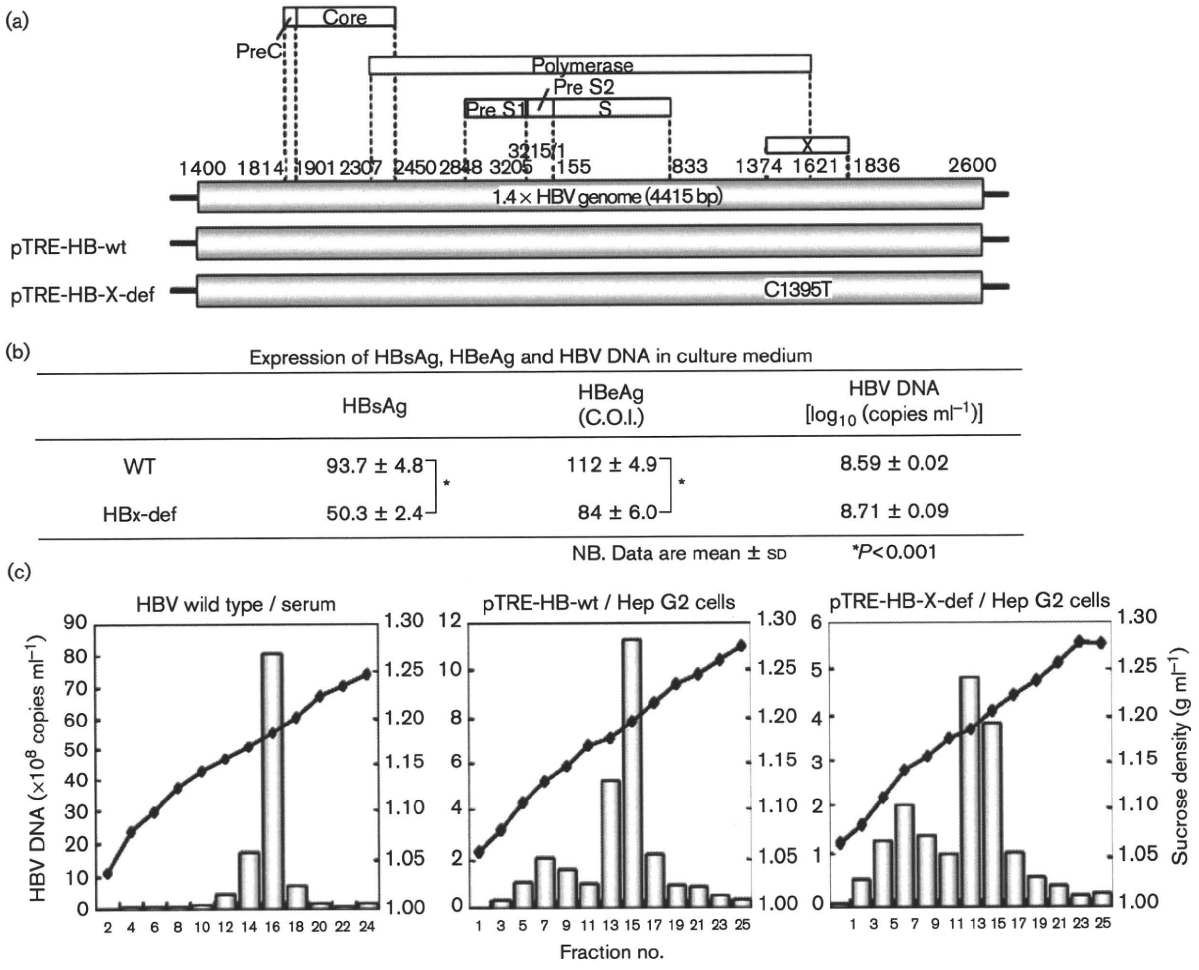

Fig. 1. Construction of HBV expression plasmids. (a) Wild type (WT) 1.4× genome length HBV was cloned into the pTRE2hyg vector (pTRE-HB-wt) and a nucleotide substitution, C1395T, was introduced to create the HBx-def mutant pTRE-HB-X-def. (b) Comparison of expression of HBsAg, HBeAg and HBV DNA in culture medium between WT and HBx-def. (c) Sucrose density gradient analysis of HBV particles (◆) and HBV DNA copies (bars) obtained from a serum sample (left) and supernatants from a cell culture transfected with WT HBV (pTRE-HB-wt, middle) and HBx-def pTRE-HB-X-def. C.O.I., cut-off index.

replication of HBV to the WT level. The effects of HBx protein were also evident on the expression of HBsAg (Fig. 3c) and HBeAg (Fig. 3d). As reported previously, the effect of the C-terminal two-thirds (aa 51–154) of the HBx protein was stronger than that of the entire protein and the N-terminal one-third (aa 1–50) (Tang *et al.*, 2005). The production of replication intermediates was increased similarly by co-transfection of the X proteins (Fig. 3e). To further study the effect of HBx expression, we analysed the levels of intracellular core protein expression. As shown in Fig. 4(a), the expression levels of the core protein were upregulated with the expression of the entire (WT) and C-terminal two-thirds (aa 51–154) of the HBx protein. Immunocytochemical analysis showed that only the cells with strong HBx protein expression were stained with the core protein (Fig. 4b). The core and HBx proteins in these cells were stained mainly in the cytoplasm.

Expression of HBx protein in mouse liver by hydrodynamic injection

Next, we expressed the HBx protein in the chimeric mouse liver with hydrodynamic injection. As shown in Fig. 5(a), a dose-dependent expression of the HBx protein with a haemagglutinin (HA) tag was confirmed by Western blot analysis. Although Henkler *et al.* (2001) showed an aggregation of HBx under the control of the human cytomegalovirus (CMV) promoter, we were able to observe expression of properly sized HBx. Immunohistochemical analysis also revealed HBx protein expression in the mouse

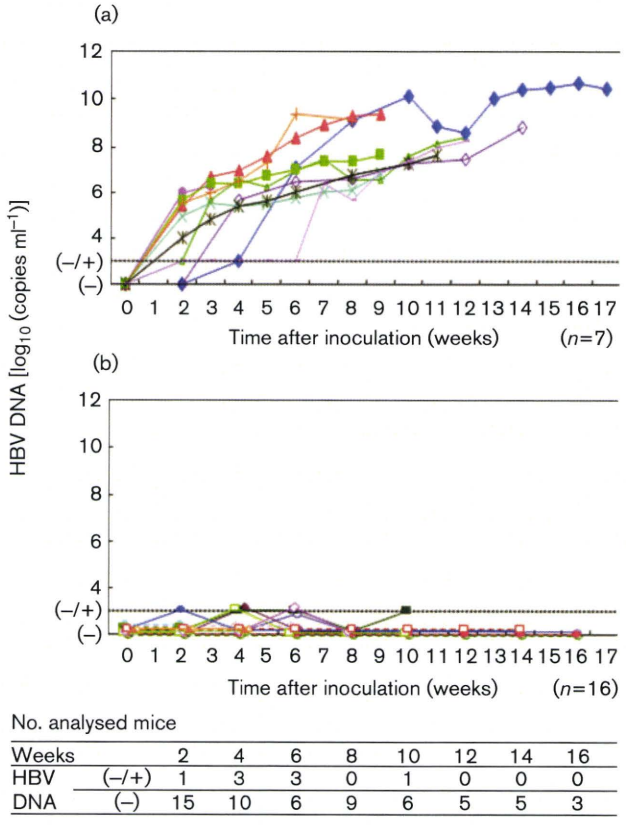

No. analysed mice

Weeks		2	4	6	8	10	12	14	16
HBV DNA	(−/+)	1	3	3	0	1	0	0	0
	(−)	15	10	6	9	6	5	5	3

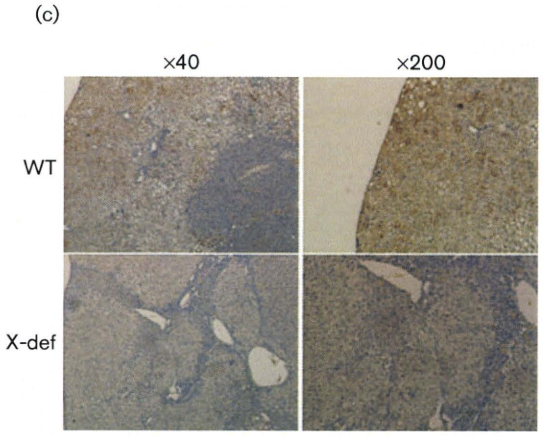

Fig. 2. Infection of human hepatocyte chimeric mice with cell-culture-derived HBV. (a, b) WT (a) and HBx-def (b) HBV particles generated from HepG2 cell lines by transfection of overlength HBV plasmid injected into chimeric mice. (c) Immunohistochemical analysis of mouse liver infected with WT (upper panel) and HBx-def (lower panel) HBV using anti-HBc antibody. HBV-infected hepatocytes were stained brown.

liver. Notably, the HBx protein staining was strong around the central vein (Fig. 5b).

Infection of HBx-def HBV particles with intrahepatic expression of the HBx protein

As the infection experiments with HBx-def HBV failed to result in measurable viraemia (Fig. 2b), we then tried to infect HBx-def HBV after expression of HBx protein by hydrodynamic injection. As shown in Fig. 6(a), six of seven mice developed measurable viraemia 2–8 weeks after inoculation. The incidence of measurable viraemia was significantly higher in mice that received hydrodynamic injection than in those without (Fig. 2b versus Fig. 6a, $P<0.0001$). Immunohistochemical analysis of the infected mice showed simultaneous staining for human serum albumin (hAlb) and HBcAg in the same portion of the liver (Fig. 6b).

Sequence analysis of inocula and the infected mouse sera

We analysed nucleotide sequences of the virus recovered from all six infected mice and compared them with those of inoculated HBx-def HBV. As shown in Fig. 7(a), direct sequencing analyses of the amplified HBV DNA products showed that all revertant viruses had T1395C (mouse MHX#1, 3, 5–7) or T1395A (mouse MHX#2) point mutations, which reverted the introduced stop codon to amino acids. We further analysed nucleotide sequences of HBV by cloning and sequencing using serum samples obtained from two mice (MHX#1, 33 clones; MHX#2, 38 clones) (Fig. 7b). Only one of 33 clones obtained from MHX#1 and none of the 38 clones from MHX#2 had the stop codon mutation that was introduced into the transfected plasmid.

DISCUSSION

In previous studies, HBx has been reported to be a multifunctional protein affecting cell growth and proliferation and activating transcription of mRNA (Arbuthnot *et al.*, 2000; Bouchard *et al.*, 2001; Klein *et al.*, 1999; Murakami, 2001) and virus replication in HCC cell lines (Bouchard *et al.*, 2001; Keasler *et al.*, 2007; Leupin *et al.*, 2005; Tang *et al.*, 2005) and mouse hepatocytes (Keasler *et al.*, 2007; Xu *et al.*, 2002). However, these results were obtained by introduction of HBV genomes into cells using artificial methods such as transfection, gene transfer and hydrodynamic injection. Recently, we established an *in vivo* HBV infection system using human hepatocyte chimeric mice (Tsuge *et al.*, 2005). The system enabled us to perform infection experiments using HBV-containing patient sera and cell-culture medium. Using this system,

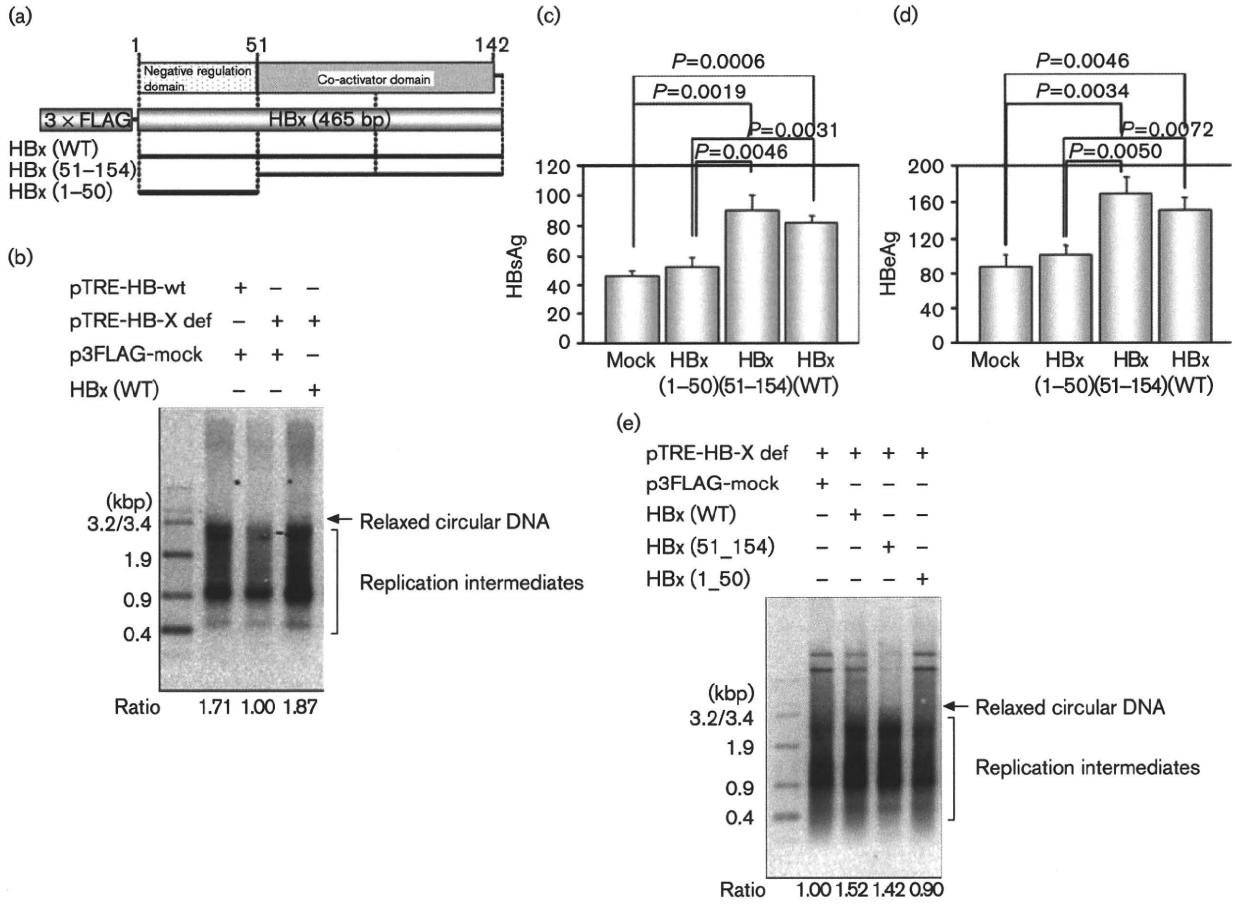

Fig. 3. Recovery of reduced formation of replication intermediate and HB antigens from HBx-def HBV by *trans*-complementation of HBx. (a) Construction of HBx expression plasmids. Full-length and deletion mutants of HBx gene were cloned into the p3FLAG-CMV10 or pcDNA3 or pcDNA3.1-3HA vector. Examples of three FLAG-tagged plasmids are shown. (b) *Trans*-complementation of HBx protein restored the reduced formation of replication intermediates of HBx-def HBV. The core-associated HBV replication intermediates were collected from HepG2 cells and detected with Southern blot hybridization with a full-length HBV probe. (c–e) Recovery of reduced production of HBsAg (c) and HBeAg (d) in culture medium and replication intermediates (e) of HBx-def HBV with *trans*-complementation of HBx expression plasmids. HBx (WT) and HBx(51–154), but not HBx(1–50), effectively enhanced the formation of HBV products. (b, e) The levels of core-associated HBV DNA are shown at the bottom of each lane. Data in (c) and (d) are mean ± SD of three experiments.

we showed previously that HBeAg is dispensable for HBV infection and active replication *in vivo* (Tsuge *et al.*, 2005). Virus replication following infection of HBV particles is quite similar to natural infection. We thus applied the system to study the function of HBx protein in this study. We also utilized hydrodynamic injection of HBx expression plasmid to *trans*-complement the defective HBx. As shown by Western blot analysis (Fig. 4a), HBx protein of the expected size was produced without development of antibody in this SCID-mouse-based model system.

This natural infection mode is quite different from previous animal studies. Virus titres of HBx-def HBV were approx. 50–99 % compared with WT HBV *in vitro* (Bouchard *et al.*, 2001; Keasler *et al.*, 2007; Leupin *et al.*, 2005; Tang *et al.*, 2005) and *in vivo* (Keasler *et al.*, 2007; Xu *et al.*, 2002). High-level HBx-def virus production seen in these experiments may be the result of expression of HBV proteins other than HBx following forced introduction of plasmids into mouse liver cells by hydrodynamic injection or transgenes. Such introduction probably resulted in virus production that is similar to *in vitro* transfection experiments using cultured cells.

In vitro experiments in this study showed that normal-density HBV particles (Fig. 1c) were produced in the absence of HBx. Curiously, the amount of HBV DNA released from the cells into the supernatant was not different between WT and HBx-def HBV, even though the

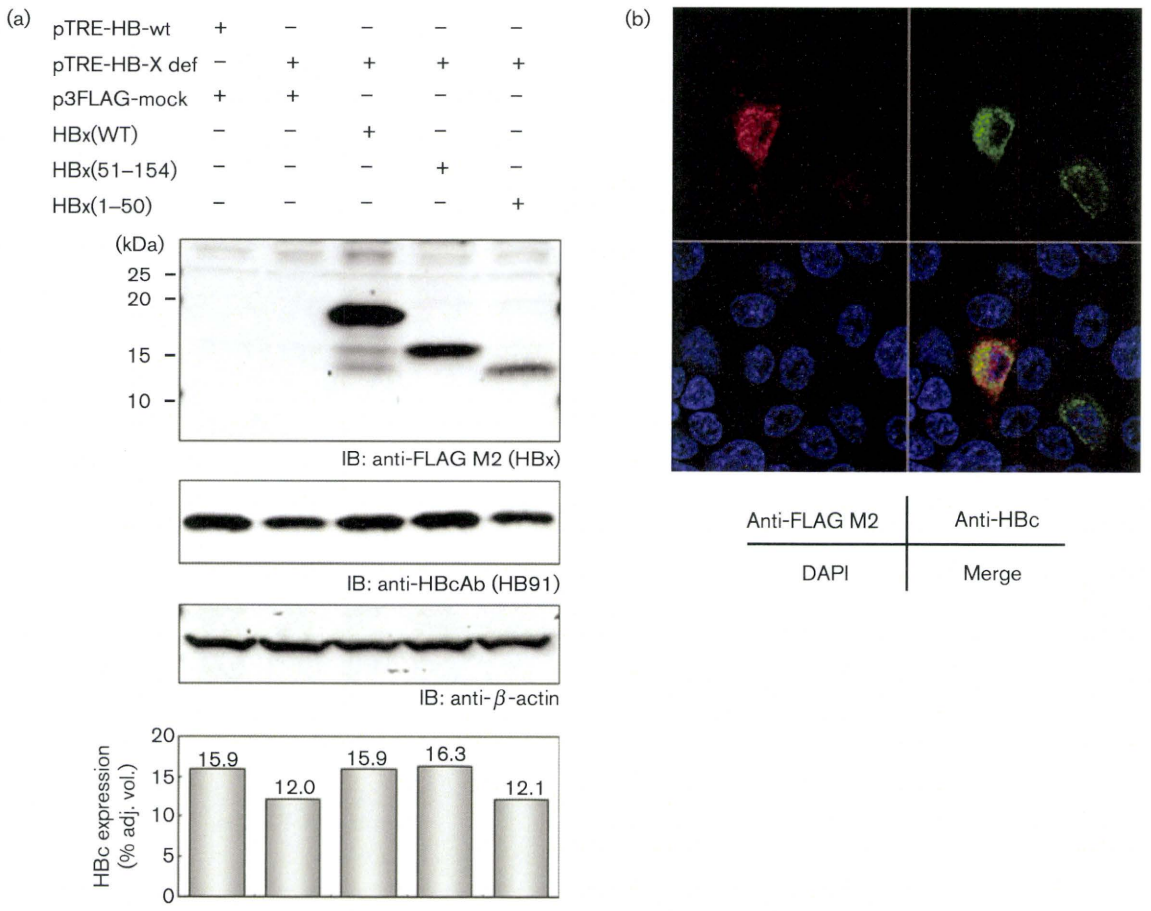

Fig. 4. Upregulation of intracellular core protein formation by *trans*-complementation of the HBx proteins. (a) Western blot analysis of intracellular proteins. Expression of the HBx proteins (percentage adjusted volume) is shown by staining the fused FLAG tag (upper panel). The membrane was also stained by the anti-HBc (middle) and anti-β-actin (lower) antibodies. Values obtained by scanning via densitometer are shown at the bottom of each lane. (b) Immunohistochemical analysis of HepG2 cells co-transfected with pTRE2-HB-X-def and p3FLAG-HBx plasmids. The expression of HBx and HBc proteins was detected by anti-FLAG (upper left) and anti-HBc (upper right) antibody, respectively. The merged image is shown in the lower right and nuclei are shown in the lower left panel. Note that only cells positive for HBx are also positive for HBc protein.

amounts of HBsAg and HBeAg as well as the amount of HBV DNA in cells were significantly greater in WT (Fig. 1b). Efficacy of release of the virus from the cells might be different between WT and HBx-def HBV. Alternatively, production of defective virus, which appeared as the second peak of HBV DNA in the sucrose gradient experiment (Fig. 1c, right panel), might be enriched in HBV DNA in the supernatant of HBx-def HBV. The reason for this discrepancy is unknown. Previous papers did not mention such production of HBV into the supernatant.

Similarly, in the absence of HBx protein *in vitro*, the formation of the replication intermediates (Fig. 3) and production of intracellular core protein (Fig. 4) continued, although their amounts were much lower. It is thus difficult to explain the inability of HBx-def HBV to infect *in vivo* simply from its transcription-activating ability, although our results confirmed that HBx has *trans*-activation ability, as reported previously (Keasler *et al.*, 2007; Tang *et al.*, 2005; Xu *et al.*, 2002). A different mode of introduction of viral nucleic acid might explain the difference seen in *in vitro* and *in vivo* experiments. In the transfection experiments, a relatively large amount of HBV DNA is introduced by transfection. In contrast, only successfully attached virus particles can introduce viral DNA into liver cells.

Strikingly, all but one (70 of 71 clones) revertant viruses had nucleotide substitutions that reversed the introduced stop codon to a coding amino acid. This is in contrast to the fact that HBV replicates in the HBx-def form in cultured cells, even though the efficacy is lower than in WT. We assumed that complemented HBx protein stimulated the replication of HBx-def HBV and increased the chance of nucleotide sequence substitutions in the HBx

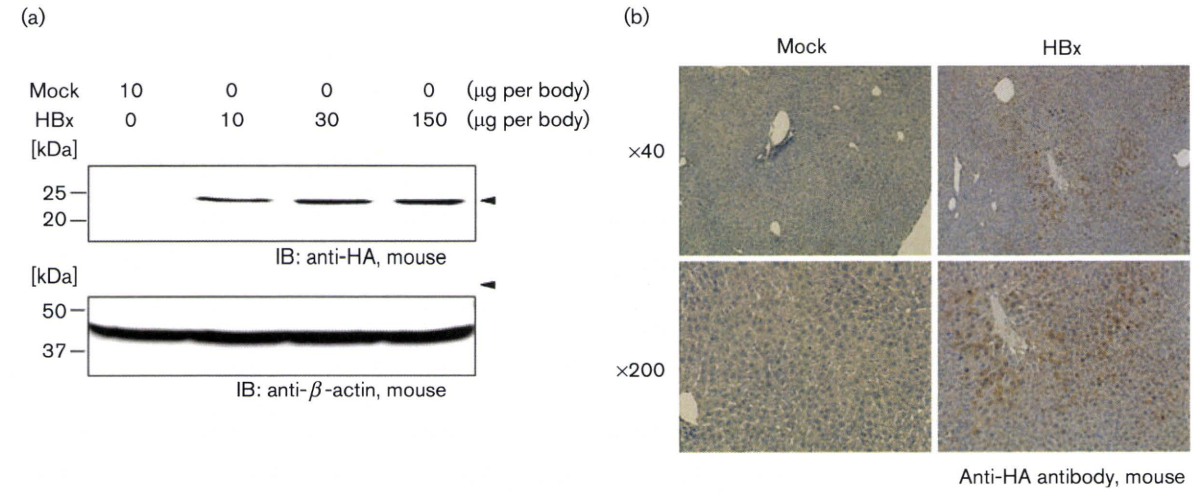

Fig. 5. Expression of HBx protein by hydrodynamic injection of HBx plasmid. (a) Liver-expressed HA-tagged HBx proteins were detected by Western blot analysis using anti-HA antibody (HA tag was used to avoid non-specific binding of anti-FLAG tag to mouse liver proteins). Dose-dependent expression of the protein was observed with different doses of the injected plasmid. (b) Immunohistochemical analysis of mouse liver using anti-HA antibody revealing expression of HBx protein. The protein was mainly expressed around the central vein.

gene, and that only revertant HBV variants predominantly increased, due to their rapid replication ability through the infection–replication cycle that only exists in the *in vivo* model. One might consider the possibility that the HBx protein works as a mutagen. However, we did not observe clear differences in the incidence of nucleotide sequence substitutions between the presence and absence of HBx (Fig. 7b and data not shown).

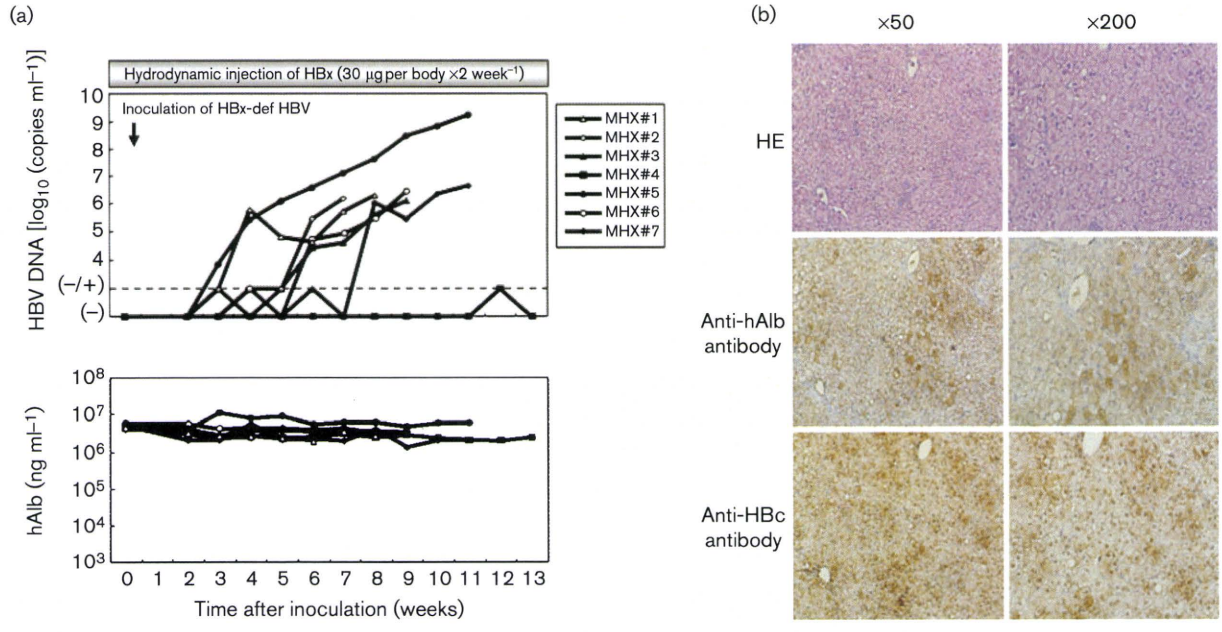

Fig. 6. Infection of HBx-def HBV particles after hydrodynamic injection of HBx expression plasmid. (a) Full-length HBx protein expression plasmid was hydrodynamically injected twice a week into human hepatocyte chimeric mice. Two weeks after the beginning of the injections, cell-culture-derived HBx-def HBV particles were injected through the tail vein. HBV DNA (upper panel) and hAlb (lower panel) were measured. (b) Immunohistochemical analysis of the infected mouse. The liver was stained with haematoxylin and eosin (HE) (upper), antibody against hAlb (middle) and anti-HBc antibody (lower).

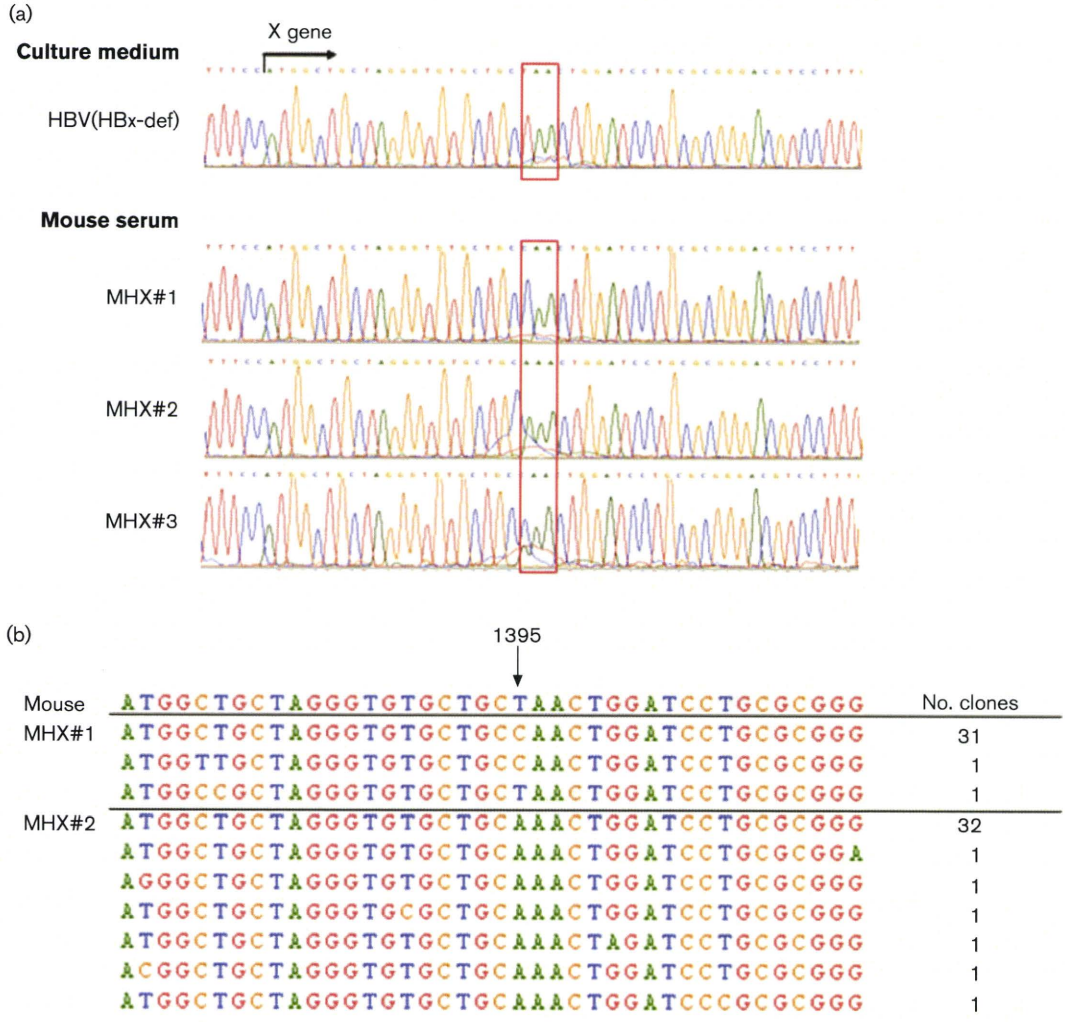

Fig. 7. Nucleotide sequence analysis of HBV recovered from HBx-def HBV-injected mice. (a) Nucleotide sequences of the HBx region of HBV determined by direct sequencing of PCR products using serum samples obtained from three mice (#1, #2 and #3 in Fig. 6a). The sequences were compared with that of inoculated HBV. Note that one of the three mice (#2) had a unique sequence different from the original sequence before introduction of the stop codon (C1395T). (b) Nucleotide sequences of the HBx gene determined by cloning and sequencing of PCR-amplified DNA from mice #1 and #2. Note that only one of 63 clones showed the introduced stop codon mutation. As we used a large amount of HBV plasmids, special care was taken to avoid contamination of DNA. Water was used as a negative control for all experiments and we observed no inappropriate amplification in these experiments.

It is thus still uncertain why the HBx protein is indispensable for virus replication *in vivo*. However, the fact that HBV cannot replicate in the absence of HBx protein may allow development of therapeutic medicine by disturbing the unknown action of HBx. To this end, it is interesting to identify a substance that binds to HBx.

The indispensability of the X protein for virus replication is a common feature shared by HBV and WHV (Chen *et al.*, 1993; Zoulim *et al.*, 1994). Both of them cause chronic infection, inflammation, fibrosis and cancer. In contrast, DHBV, which can replicate without DHBx expression, does not cause such a pathological situation (Meier *et al.*, 2003). Further analysis of the X protein may pave the way to clarify the mechanism of cancer development caused by HBV infection.

METHODS

Human hepatocyte chimeric mice experiments. Care of $uPA^{+/+}/SCID^{+/+}$ mice and transplantation of human hepatocytes were performed as described previously (Tateno *et al.*, 2004). The experiments were performed in accordance with the guidelines of the local committee for animal experiments at Hiroshima University. Infection, extraction of serum samples and sacrifice were performed under ether anaesthesia as described previously (Tateno *et al.*, 2004).

hAlb in mouse serum was measured with a Human Albumin ELISA Quantification kit (Bethyl Laboratories Inc.) according to the instructions provided by the manufacturer. Serum samples obtained from mice were aliquotted and stored in liquid nitrogen until use.

Analysis of HBV markers. HBsAg and HBeAg were measured using a commercially available ELISA kit (Abbott). For quantitative analysis of HBV DNA, 10 μl mouse serum sample or 100 μl of culture supernatant was used. DNA was extracted from these samples using the SMITEST R&D (Genome Science Laboratories) and dissolved in 20 μl H_2O, and HBV DNA was quantified by real-time PCR using the 7300 Real-Time PCR System (Applied Biosystems). Amplification was performed as described previously (Tsuge *et al.*, 2005). The lower detection limit of this assay is 300 copies. For detection of small amounts of HBV DNA, we also performed nested PCR. The amplification conditions were as described previously (Tsuge *et al.*, 2005).

Plasmid construction. The construction of wild-type (WT) HBV 1.4 genome length, pTRE-HB-wt, was described previously (Tsuge *et al.*, 2005). We used pTRE2 vector without pTet-off vector and doxycycline because a sufficient amount of HBV transcripts was produced from internal HBV promoters, and transcription from the pTRE2 promoter is negligible under these conditions. The nucleotide sequence of the HBV genome that we cloned into plasmid pTRE-HB-wt was deposited in GenBank under accession number AB206817. A modified plasmid, pTRE-HB-X-def, was generated by introducing a C-to-T point mutation at nt 1395 (aa 7) to create a stop codon (CAA to TAA) in the HBx gene (Fig. 1a). The substitution was introduced by using a QuikChange Site-Directed Mutagenesis kit (Stratagene). For the construction of the HBx gene expression plasmid, the HBx gene was amplified from pTRE-HB-wt and cloned into pcDNA3, pcDNA3-3 × HA, p3 × FLAG-CMV10 vectors and designated pcDNA-HBx, pcDNA3-HA-HBx, p3FLAG-HBx, respectively. Partially truncated HBx plasmids, with a deletion of the N-terminal 50 aa [HBx(51–154)] and the C-terminal 50 aa [HBx(1–50)], were also cloned into pcDNA3 or p3FLAG-CMV10 vectors.

Transfection of HepG2 cell lines with HBV expression plasmids. HepG2 cells were grown in Dulbecco's modified Eagle's medium supplemented with 10 % (v/v) fetal bovine serum at 37 °C and under 5 % CO_2. For functional analysis of the HBx protein *in vitro*, the HBV or HBx-def HBV expression plasmid was transfected with/without HBx expression plasmid using *Trans*IT-LT1 (Mirus) reagent according to the instructions provided by the supplier. Three to five days after transfection, core-associated HBV DNA was extracted from cells for HBV DNA quantification (Noguchi *et al.*, 2005). For analysing the infectivity of recombinant HBV particles, HBV expression plasmids were transiently transfected into HepG2 cells. The cells were seeded to semi-confluence in 90 mm dishes. WT HBV particles were generated from cells transfected with 20 μg pTRE2-HB-wt by calcium phosphate precipitation. HBx-def HBV particles were also generated from cells co-transfected with 10 μg pTRE2-HB-X-def and 10 μg pcDNA-HBx. Three days after transfection, the culture medium was collected and stored in liquid nitrogen until use.

Analysis of cell-culture-produced HBV by sucrose density gradient sedimentation. Five millilitres of HBV-positive human serum (8 $\log_{10}$ copies ml^{-1}) or 50 ml cell culture supernatant (8 $\log_{10}$ copies ml^{-1}) was layered on a 20 % (w/w) sucrose cushion, and centrifuged at 24 000 r.p.m. (maximum 103 864 *g*) for 12 h at 4 °C with a Beckman SW28 rotor (Beckman Coulter). The precipitate was resuspended in 500 μl PBS. These HBV samples were layered on a linear 20–50 % (w/w) sucrose gradient. Centrifugation was carried out at 24 000 r.p.m. (maximum 102 445 *g*) for 21 h at 4 °C with a Beckman SW40 rotor. The gradients were fractionated into 500 μl samples, and the density of each fraction was calculated from the weight and volume. Each fraction was diluted 10-fold and tested for HBV DNA by real-time PCR.

Analysis of replication intermediate of HBV. The cells were harvested 5 days after transfection and lysed with 250 μl lysis buffer [10 mM Tris/HCl (pH 7.4), 140 mM NaCl and 0.5 % (v/v) NP-40] followed by centrifugation for 2 min at 15 000 *g*. The core-associated HBV genome was immunoprecipitated by mouse anti-HBV core monoclonal antibody 2A21 (Institute of Immunology, Tokyo, Japan) and subjected to Southern blot analysis after SDS/proteinase K digestion, followed by phenol extraction and ethanol precipitation. Quantitative analysis was performed by real-time PCR with SYBR Green using the 7300 Real-Time PCR System and the amounts of the replication intermediates were compared. The HBV-specific primers used for amplification were 5′-TTTGGGCATGGACATTGAC-3′ and 5′-GGTGAACAATGTTCCGGAGAC-3′. The amplification conditions included initial denaturation at 95 °C for 10 min, followed by 45 cycles of denaturation at 95 °C for 15 s, annealing at 58 °C for 5 s and extension at 72 °C for 6 s. The lower detection limit of this assay was 300 copies.

Immunocytochemistry of HepG2 cells transfected with pTRE2-HB-X-def and p3FLAG-HBx plasmids. HepG2 cells were seeded to semi-confluence in two-well chamber plates. Each 1 μg pTRE2-HB-X-def and p3FLAG-HBx plasmids was co-transfected using *Trans*IT-LT1 reagent (Mirus) according to the instructions provided by the supplier. The cells were harvested 24 h after transfection and then washed with PBS and fixed with 4 % (v/v) paraformaldehyde. After fixation, the cells were stained with mouse monoclonal antibody directed to FLAG (Sigma) or rabbit polyclonal antibody against hepatitis B core antigen (HBcAg; DAKO Diagnostika) as the primary antibody. The bound antibodies were detected with an Alexa Fluor 488-conjugated antibody against rabbit IgG or Alexa Fluor 568-conjugated antibody against mouse IgG, respectively (Molecular Probes). Nuclei were counterstained with 6-diamidino-2-phenylindole (DAPI) (Vector Laboratories).

Hydrodynamic injection of HBx expression plasmids. Hydrodynamic injection was performed as reported previously (Yang *et al.*, 2002) with slight modifications. As the human hepatocyte chimeric mice were quite small (12–15 g) and weak for the rapid injection and the stress, we reduced the amount of DNA solution and injection speed: 1 ml PBS containing 30 μg HBx expression plasmids was injected rapidly through the mouse tail vein within 30 s. For analysis of infectivity of HBx-def HBV particles, the plasmids were injected twice a week.

Western blot analysis. Mouse liver tissues or transfected HepG2 cells were cooled on ice and treated with RIPA-like buffer [50 mM Tris/HCl (pH 8.0), 0.1 % SDS, 1 % NP-40, 150 mM sodium chloride and 0.5 % sodium deoxycholate] containing protease inhibitor cocktail (Sigma). Cell lysates were separated on SDS–polyacrylamide gels [5–20 % (w/v)] (Bio-Rad) and then transferred onto nitrocellulose membranes (GE Healthcare) by electroblotting. The membranes were incubated with anti-haemagglutinin fusion epitope (anti-HA) monoclonal antibody (Roche) or with anti β-actin monoclonal antibody (Sigma) followed by incubation with horseradish peroxidase-conjugated sheep anti-mouse immunoglobulin (GE Healthcare). Proteins were visualized via the ChemiDoc XRS system (Bio-Rad). Expression of HBc protein was quantified from the densities of the immunoblot signals by Quantity One software (Bio-Rad).

Immunohistochemical analysis of mouse liver. The liver specimens of HBV-infected mice were fixed with 10 % buffered paraformaldehyde and embedded in paraffin blocks for histological

examination. The liver sections were stained with haematoxylin–eosin or subjected to immunohistochemical staining using an antibody against HBcAg (DAKO Diagnostika), anti-HA antibody or HSA (Bethyl Laboratories Inc.). Endogenous peroxidase activity was blocked with 0.3 % H_2O_2 and methanol. Immunoreactive materials were visualized by using a streptavidin–biotin staining kit (Histofine SAB-PO kit; Nichirei) and diaminobenzidine.

Sequence analysis of the HBV genome. Genome-length HBV DNA was amplified by PCR as described by Günther *et al.* (1995). HBV genome-length PCR products were subjected to 1 % agarose gel electrophoresis and the 3.2 kbp band was extracted using a QiaEx II Gel Extraction kit (Qiagen). Direct sequencing, cloning and sequencing (Ohishi *et al.*, 2004) were performed in an ABI PRISM 3100-Avant Genetic Analyzer (Applied Biosystems) with a Big Dye Terminator version 3.0 Cycle Sequencing Ready Reaction kit (Applied Biosystems).

Statistical analysis. All data are expressed as mean ± SD. Differences between groups were examined for statistical significance by using Student's *t*-test. A *P* value <0.05 denoted the presence of a statistically significant difference.

ACKNOWLEDGEMENTS

This work was carried out at the Research Center for Molecular Medicine, Faculty of Medicine, Hiroshima University, and the Analysis Center of Life Science, Hiroshima University. The authors thank Chiemi Noguchi and Waka Ohishi for their helpful discussion, Kana Kunihiro for her excellent technical assistance, and Yoshiko Nakata and Aya Furukawa for secretarial assistance. Financial support was provided by the Ministry of Education, Sports, Culture and Technology and Ministry of Health, Labour and Welfare (Grants-in-Aid for scientific research and development).

REFERENCES

Ando, T., Sugiyama, K., Goto, K., Miyake, Y., Li, R., Kawabe, Y. & Wada, Y. (1999). Age at time of hepatitis Be antibody seroconversion in childhood chronic hepatitis B infection and mutant viral strain detection rates. *J Pediatr Gastroenterol Nutr* **29**, 583–587.

Arbuthnot, P., Capovilla, A. & Kew, M. (2000). Putative role of hepatitis B virus X protein in hepatocarcinogenesis: effects on apoptosis, DNA repair, mitogen-activated protein kinase and JAK/STAT pathways. *J Gastroenterol Hepatol* **15**, 357–368.

Bouchard, M. J., Wang, L. H. & Schneider, R. J. (2001). Calcium signaling by HBx protein in hepatitis B virus DNA replication. *Science* **294**, 2376–2378.

Chen, H. S., Kaneko, S., Girones, R., Anderson, R. W., Hornbuckle, W. E., Tennant, B. C., Cote, P. J., Gerin, J. L., Purcell, R. H. & Miller, R. H. (1993). The woodchuck hepatitis virus X gene is important for establishment of virus infection in woodchucks. *J Virol* **67**, 1218–1226.

Colgrove, R., Simon, G. & Ganem, D. (1989). Transcriptional activation of homologous and heterologous genes by the hepatitis B virus X gene product in cells permissive for viral replication. *J Virol* **63**, 4019–4026.

Dandri, M., Schirmacher, P. & Rogler, C. E. (1996). Woodchuck hepatitis virus X protein is present in chronically infected woodchuck liver and woodchuck hepatocellular carcinomas which are permissive for viral replication. *J Virol* **70**, 5246–5254.

Dandri, M., Petersen, J., Stockert, R. J., Harris, T. M. & Rogler, C. E. (1998). Metabolic labeling of woodchuck hepatitis B virus X protein in naturally infected hepatocytes reveals a bimodal half-life and association with the nuclear framework. *J Virol* **72**, 9359–9364.

Doria, M., Klein, N., Lucito, R. & Schneider, R. J. (1995). The hepatitis B virus HBx protein is a dual specificity cytoplasmic activator of Ras and nuclear activator of transcription factors. *EMBO J* **14**, 4747–4757.

Ganem, D. & Schneider, R. J. (2001). *Hepadnaviridae*: the viruses and their replication. In *Fields Virology*, 4th edn, pp. 2923–2969. Edited by D. M. Knipe, P. M. Howley, D. E. Griffin, R. A. Lamb, M. A. Martin, B. Roizman & S. E. Straus. Philadelphia, PA: Lippincott Williams & Wilkins.

Günther, S., Li, B. C., Miska, S., Kruger, D. H., Meisel, H. & Will, H. (1995). A novel method for efficient amplification of whole hepatitis B virus genomes permits rapid functional analysis and reveals deletion mutants in immunosuppressed patients. *J Virol* **69**, 5437–5444.

Henkler, F., Hoare, J., Waseem, N., Goldin, R. D., McGarvey, M. J., Koshy, R. & King, I. A. (2001). Intracellular localization of the hepatitis B virus HBx protein. *J Gen Virol* **82**, 871–882.

Jacob, J. R., Ascenzi, M. A., Roneker, C. A., Toshkov, I. A., Cote, P. J., Gerin, J. L. & Tennant, B. C. (1997). Hepatic expression of the woodchuck hepatitis virus X-antigen during acute and chronic infection and detection of a woodchuck hepatitis virus X-antigen antibody response. *Hepatology* **26**, 1607–1615.

Keasler, V. V., Hodgson, A. J., Madden, C. R. & Slagle, B. L. (2007). Enhancement of hepatitis B virus replication by the regulatory X protein *in vitro* and *in vivo*. *J Virol* **81**, 2656–2662.

Klein, N. P., Bouchard, M. J., Wang, L. H., Kobarg, C. & Schneider, R. J. (1999). Src kinases involved in hepatitis B virus replication. *EMBO J* **18**, 5019–5027.

Leupin, O., Bontron, S., Schaeffer, C. & Strubin, M. (2005). Hepatitis B virus X protein stimulates viral genome replication via a DDB1-dependent pathway distinct from that leading to cell death. *J Virol* **79**, 4238–4245.

Meier, P., Scougall, C. A., Will, H., Burrell, C. J. & Jilbert, A. R. (2003). A duck hepatitis B virus strain with a knockout mutation in the putative X ORF shows similar infectivity and *in vivo* growth characteristics to wild-type virus. *Virology* **317**, 291–298.

Melegari, M., Wolf, S. K. & Schneider, R. J. (2005). Hepatitis B virus DNA replication is coordinated by core protein serine phosphorylation and HBx expression. *J Virol* **79**, 9810–9820.

Mercer, D. F., Schiller, D. E., Elliott, J. F., Douglas, D. N., Hao, C., Rinfret, A., Addison, W. R., Fischer, K. P., Churchill, T. A. & other authors (2001). Hepatitis C virus replication in mice with chimeric human livers. *Nat Med* **7**, 927–933.

Murakami, S. (2001). Hepatitis B virus X protein: a multifunctional viral regulator. *J Gastroenterol* **36**, 651–660.

Noguchi, C., Ishino, H., Tsuge, M., Fujimoto, Y., Imamura, M., Takahashi, S. & Chayama, K. (2005). G to A hypermutation of hepatitis B virus. *Hepatology* **41**, 626–633.

Ohishi, W., Shirakawa, H., Kawakami, Y., Kimura, S., Kamiyasu, M., Tazuma, S., Nakanishi, T. & Chayama, K. (2004). Identification of rare polymerase variants of hepatitis B virus using a two-stage PCR with peptide nucleic acid clamping. *J Med Virol* **72**, 558–565.

Raney, A. K. & McLachlan, A. (1991). The biology of hepatitis B virus. In *Molecular Biology of the Hepatitis B Virus*, pp. 1–37. Edited by A. McLachlan. Boca Raton, FL: CRC Press.

Seeger, C. & Mason, W. S. (2000). Hepatitis B virus biology. *Microbiol Mol Biol Rev* **64**, 51–68.

Sitterlin, D., Bergametti, F., Tiollais, P., Tennant, B. C. & Transy, C. (2000a). Correct binding of viral X protein to UVDDB-p127 cellular protein is critical for efficient infection by hepatitis B viruses. *Oncogene* **19**, 4427–4431.

Sitterlin, D., Bergametti, F. & Transy, C. (2000b). UVDDB p127-binding modulates activities and intracellular distribution of hepatitis B virus X protein. *Oncogene* **19**, 4417–4426.

Su, Q., Schroder, C. H., Hofmann, W. J., Otto, G., Pichlmayr, R. & Bannasch, P. (1998). Expression of hepatitis B virus X protein in HBV-infected human livers and hepatocellular carcinomas. *Hepatology* **27**, 1109–1120.

Tang, H., Banks, K. E., Anderson, A. L. & McLachlan, A. (2001). Hepatitis B virus transcription and replication. *Drug News Perspect* **14**, 325–334.

Tang, H., Delgermaa, L., Huang, F., Oishi, N., Liu, L., He, F., Zhao, L. & Murakami, S. (2005). The transcriptional transactivation function of HBx protein is important for its augmentation role in hepatitis B virus replication. *J Virol* **79**, 5548–5556.

Tateno, C., Yoshizane, Y., Saito, N., Kataoka, M., Utoh, R., Yamasaki, C., Tachibana, A., Soeno, Y., Asahina, K. & other authors (2004). Near completely humanized liver in mice shows human-type metabolic responses to drugs. *Am J Pathol* **165**, 901–912.

Tsuge, M., Hiraga, N., Takaishi, H., Noguchi, C., Oga, H., Imamura, M., Takahashi, S., Iwao, E., Fujimoto, Y. & other authors (2005). Infection of human hepatocyte chimeric mouse with genetically engineered hepatitis B virus. *Hepatology* **42**, 1046–1054.

Wang, W. L., London, W. T. & Feitelson, M. A. (1991). Hepatitis B X antigen in hepatitis B virus carrier patients with liver cancer. *Cancer Res* **51**, 4971–4977.

Xu, Z., Yen, T. S., Wu, L., Madden, C. R., Tan, W., Slagle, B. L. & Ou, J. H. (2002). Enhancement of hepatitis B virus replication by its X protein in transgenic mice. *J Virol* **76**, 2579–2584.

Yang, P. L., Althage, A., Chung, J. & Chisari, F. V. (2002). Hydrodynamic injection of viral DNA: a mouse model of acute hepatitis B virus infection. *Proc Natl Acad Sci U S A* **99**, 13825–13830.

Zhang, Z., Torii, N., Hu, Z., Jacob, J. & Liang, T. J. (2001). X-deficient woodchuck hepatitis virus mutants behave like attenuated viruses and induce protective immunity *in vivo*. *J Clin Invest* **108**, 1523–1531.

Zoulim, F., Saputelli, J. & Seeger, C. (1994). Woodchuck hepatitis virus X protein is required for viral infection *in vivo*. *J Virol* **68**, 2026–2030.

Journal of General Virology (2010), **91**, 1668–1677 DOI 10.1099/vir.0.019315-0

Practical evaluation of a mouse with chimeric human liver model for hepatitis C virus infection using an NS3-4A protease inhibitor

Naohiro Kamiya,[1] Eiji Iwao,[1] Nobuhiko Hiraga,[2,3] Masataka Tsuge,[2,3] Michio Imamura,[2,3] Shoichi Takahashi,[2,3] Shinji Miyoshi,[4] Chise Tateno,[3,5] Katsutoshi Yoshizato[3,5] and Kazuaki Chayama[2,3]

Correspondence
Kazuaki Chayama
chayama@hiroshima-u.ac.jp

[1]Pharmacology Department V, Mitsubishi Tanabe Pharma Corporation, Yokohama, Japan

[2]Department of Medicine and Molecular Science, Division of Frontier Medical Science, Programs for Biomedical Research, Graduate School of Biomedical Sciences, Hiroshima University, Hiroshima, Japan

[3]Liver Research Project Center, Hiroshima University, Hiroshima, Japan

[4]DMPK Department, Mitsubishi Tanabe Pharma Corporation, Kisarazu, Chiba, Japan

[5]PhoenixBio, Higashihiroshima, Japan

A small-animal model for hepatitis C virus (HCV) infection was developed using severe combined immunodeficiency (SCID) mice encoding homozygous urokinase-type plasminogen activator (uPA) transplanted with human hepatocytes. Currently, limited information is available concerning the HCV clearance rate in the SCID mouse model and the virion production rate in engrafted hepatocytes. In this study, several cohorts of $uPA^{+/+}/SCID^{+/+}$ mice with nearly half of their livers repopulated by human hepatocytes were infected with HCV genotype 1b and used to evaluate HCV dynamics by pharmacokinetic and pharmacodynamic analyses of a specific NS3-4A protease inhibitor (telaprevir). A dose-dependent reduction in serum HCV RNA was observed. At telaprevir exposure equivalent to that in clinical studies, rapid turnover of serum HCV was also observed in this mouse model and the estimated slopes of virus decline were 0.11–0.17 $\log_{10}$ h^{-1}. During the initial phase of treatment, the $\log_{10}$ reduction level of HCV RNA was dependent on the drug concentration, which was about fourfold higher in the liver than in plasma. HCV RNA levels in the liver relative to human endogenous gene expression were correlated with serum HCV RNA levels at the end of treatment for up to 10 days. A mathematical model analysis of viral kinetics suggested that 1 g of the chimeric human liver could produce at least 10^8 virions per day, and this may be comparable to HCV production in the human liver.

Received 17 December 2009
Accepted 17 February 2010

INTRODUCTION

Hepatitis C virus (HCV) is a major cause for concern worldwide. More than 3 % of the world's population is chronically infected with HCV and 3–4 million people are newly infected each year (Wasley & Alter, 2000). Chronic HCV infection is relatively mild and progresses slowly; however, about 20 % of chronic hepatitis C (CHC) carriers progress to serious end-stage liver disease (Lauer & Walker, 2001; Liang *et al.*, 2000; Poynard *et al.*, 2003). The current standard treatment for HCV infection is administration of pegylated alpha interferon (PEG-IFN) in combination with ribavirin (RBV) for 48 weeks. The overall cure rates with this intervention are 40–50 % for patients with genotype 1 and more than 75 % for patients with genotypes 2 and 3 (Fried *et al.*, 2002; Manns *et al.*, 2001). Several compounds that inhibit specific stages of the virus life cycle have been clinically evaluated (Manns *et al.*, 2007; Pereira & Jacobson, 2009). Telaprevir is a novel peptidomimetic slow- and tight-binding inhibitor of HCV NS3-4A protease, which was discovered using a structure-based drug design approach (Perni *et al.*, 2006). A rapid decline in viral RNA was observed in CHC patients treated with telaprevir (Reesink *et al.*, 2006) and an increased antiviral effect of a combination of telaprevir and PEG-IFN has been reported (Forestier *et al.*, 2007). Recent clinical trials of telaprevir in combination with PEG-IFN and RBV have indicated a promising material advance in therapy for CHC patients (Hézode *et al.*, 2009; McHutchison *et al.*, 2009). First-generation HCV-specific agents have been developed despite the lack of small-animal models for HCV infection. However, early emergence of resistant variants against novel antiviral agents is a concern. Thus, the use of two or more investigation agents is strongly recommended for

clinical studies in CHC patients (Sherman *et al.*, 2007). To ensure ethical and safe clinical trials, animal models continue to be necessary for the mechanistic evaluation of the ability of specific agents to inhibit the virus life cycle *in vivo* and to develop better therapeutic strategies, including combination regimens (Boonstra *et al.*, 2009). Several groups have developed a small-animal model for HCV infection using homozygous urokinase-type plasminogen activator (uPA)/severe combined immunodeficiency (SCID) ($uPA^{+/+}/SCID^{+/+}$) mice transplanted with human hepatocytes (Mercer *et al.*, 2001). These mice are susceptible to cell culture-grown HCV (HCVcc; Lindenbach *et al.*, 2006) and have been used to evaluate antiviral agents including IFN-α, BILN 2061 (an NS3-4A protease inhibitor) and HCV796 (an NS5B polymerase inhibitor) (Kneteman *et al.*, 2006, 2009; Vanwolleghem *et al.*, 2007). However, the HCV clearance rate in the SCID mouse model and the virion production rate in hepatocytes engrafted in the mouse liver are not fully understood. We also generated a mouse model with an almost humanized liver (Tateno *et al.*, 2004). Using this mouse model, we reported the infection of a genetically engineered hepatitis B virus (Tsuge *et al.*, 2005) and developed a reverse genetics system for HCV genotypes 1a, 1b and 2a after intrahepatic injection of *in vitro*-transcribed RNA as well as intravenous injection of HCVcc (Hiraga *et al.*, 2007; Kimura *et al.*, 2008). In this study, we demonstrated the rapid turnover of serum HCV RNA and the pharmacokinetics (PK) and pharmacodynamics (PD) of telaprevir treatment. We concluded after quantitative estimation and the use of a mathematical model that HCV production equivalent to that in the human liver is possible in engrafted hepatocytes in this mouse model.

RESULTS

Preliminary dose-finding study

At the beginning of this study, we attempted to determine an effective dose regimen for telaprevir in this mouse model. Nine mice were randomized and treated with telaprevir over three time periods (Table 1). The lifetime kinetics of serum HCV RNA and of human serum albumin (HSA) in blood are represented in Fig. 1. One mouse (A07) exhibited a rapid reduction in HSA in the blood, which indicated the instability of human hepatocyte grafts. As a rapid reduction in HSA levels was not observed in subsequent experiments, this mouse was excluded from the mean analysis. After 7 days of twice daily (BID) dosing in period 1, the mean $\log_{10}$ changes in HCV RNA from baseline ($\pm$SEM) after the 100 and 10 mg telaprevir kg^{-1} doses were -0.49 ± 0.094 and -0.53 ± 0.039, respectively, and no dose-dependent reduction was observed. During period 2, the dose frequency was changed from BID to three times daily (TID), and the time of serum sampling was also changed from 1 to 4 h after the last dose. After the 3-day treatment, the mean $\log_{10}$ changes of HCV RNA in 100 and 10 mg telaprevir kg^{-1} TID groups were -1.00 ± 0.166 and -0.28 ± 0.056, respectively, and the difference between the two groups was significant. To test the reproducibility of results, mice were treated with 10 or 100 mg telaprevir kg^{-1} TID for 10 days and then sacrificed 5 h after the administration of the last dose. The mean $\log_{10}$ changes in serum HCV RNA were -1.46 ± 0.265 and -0.27 ± 0.073 in the 100 and 10 mg kg^{-1} TID groups, respectively, and the difference between the means was significant.

Evaluation of HCV turnover in this mouse model

Because of the SCID nature of this mouse model, the virion clearance mechanism was of interest. Six mice with steady-state and high viral loads (9.7×10^5–1.2×10^8 copies ml^{-1}) were administered 200 mg telaprevir kg^{-1} TID for 4 days, with 5 h intervals between doses and a 14 h intermission from drug treatment each day. Because the $\log_{10}$ reduction in HCV RNA appeared to depend on the time of serum collection during the day (Fig. 2a), the mean $\log_{10}$ changes in HCV RNA were plotted against time and fitted to a linear regression model (Fig. 2b). The estimated slopes (i.e. $\log_{10}$ HCV reduction per hour) and 95% confidence intervals (CI) on days 1, 2 and 3 were -0.165 (-0.268 to 0.0616), -0.115 (-0.131 to 0.0990) and -0.153, respectively. These regression lines also suggested that extrapolated HCV loads at the actual times of the daily first doses were 0.0530, -0.220 and -0.0948 $\log_{10}$ copies ml^{-1}, respectively. Therefore, it appeared that the viral load

Table 1. Telaprevir dose-finding experiment

Period	Duration (days)	Frequency of dose (per day)	Dose (mg kg^{-1})	No. of mice	Mean $\log_{10}$ changes ± SEM	*P* value (*t* test)
1	7	2	100	4	-0.49 ± 0.094	0.7806
			10	3*	-0.53 ± 0.039	
			0	1	-0.47	
2	3	3	100	4*	-1.00 ± 0.166	0.0064
			10	4	-0.28 ± 0.056	
3	10	3	100	3	-1.46 ± 0.265	0.0125
			10	3	-0.27 ± 0.073	

*One mouse was excluded because of instability of human hepatocyte grafts.

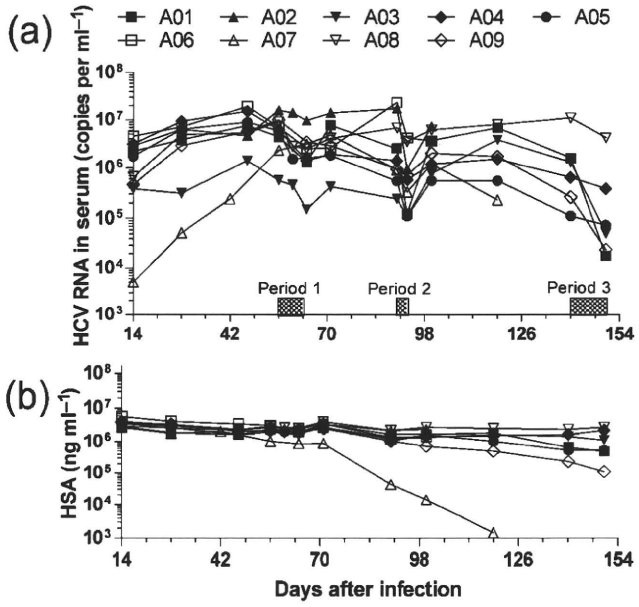

Fig. 1. Lifelong changes in serum HCV RNA and HSA in the blood of HCV-infected mice in the preliminary dose-finding experiment. Nine HCV-infected mice (A01–A09) were treated with telaprevir over three independent periods. The mice were treated with 10 mg telaprevir kg^{-1}, 100 mg telaprevir kg^{-1} or vehicle BID for 7 days (period 1), TID for 3 days (period 2) and TID for 10 days (period 3). (a) Kinetics of serum HCV RNA. (b) Kinetics of HSA level in blood. Because the HSA level indicated the stability of engrafted human hepatocytes in the mice, mouse A07 was excluded from the summary of the results in Table 1.

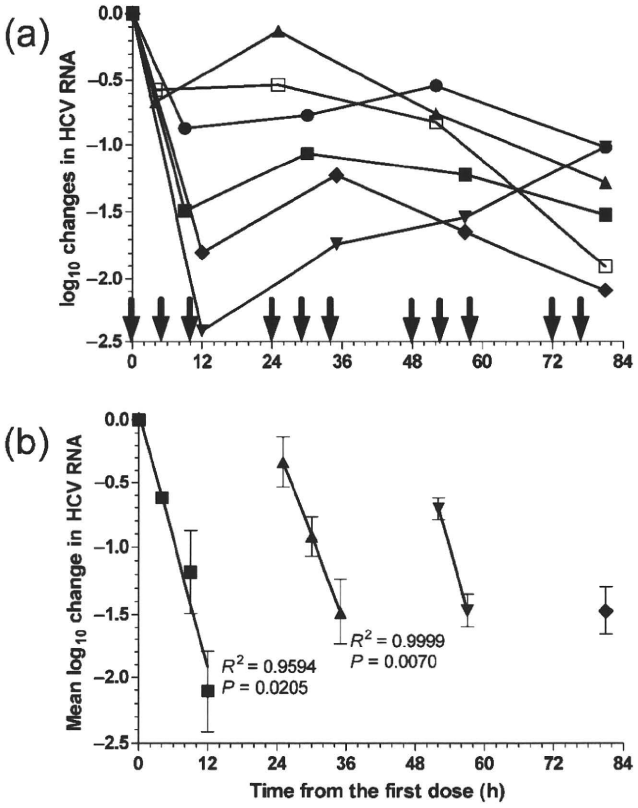

Fig. 2. Estimation of virus clearance rate. Six HCV-infected mice were treated with 200 mg telaprevir kg^{-1} TID for 4 days. Individual kinetics of $\log_{10}$ reductions in serum HCV RNA (a) and of mean $\log_{10}$ changes (±SEM) at each sampling time (b) are represented. Arrows indicate the times of dosing. The slopes of mean $\log_{10}$ HCV RNA reduction were estimated by linear regression analysis. P and R^2 values are indicated on the figure.

reverted back towards baseline levels during the 14 h intermission from drug treatment.

PK analysis

To assess drug exposure after repeated dosing in this mouse model, mice were administered 100 or 300 mg telaprevir kg^{-1} BID for 4 days. The mice receiving 300 mg kg^{-1} BID for 4 days had a mean 2 $\log_{10}$-fold HCV reduction, whereas those receiving 100 mg kg^{-1} BID had up to a 1.5 $\log_{10}$-fold reduction by day 3 (Fig. 3a). Plasma telaprevir concentrations after administration of the final dose are indicated in Fig. 3(b). The estimated half-life of telaprevir in the 100 and 300 mg kg^{-1} groups was 2.4 and 3.8 h, respectively.

PK/PD analysis and the dose-dependent reduction in HCV RNA

To evaluate the correlation between telaprevir concentration and HCV reductions in this mouse model, we used another cohort of 12 HCV-infected mice with high viral loads (1.6×10^6–3.9×10^8 copies ml^{-1}). In this crossover study, mice were randomized into three groups (n=4 each), each of which underwent two periods of dosing for 5 days separated by a 1-week washout period. Serum and plasma samples were collected once daily 5 h after dosing. The mean $\log_{10}$ changes in HCV RNA (±SEM) at different dose levels were calculated from the combined results of both periods (Fig. 4a). The mean $\log_{10}$ reductions from baseline in the 100 and 300 mg kg^{-1} groups were approximately 1 $\log_{10}$ and 1.5–2 $\log_{10}$, respectively, and the difference between the two groups was statistically significant. The means calculated in each period separately are also shown in Fig. 4(b). The plasma telaprevir concentration was positively correlated with the $\log_{10}$ HCV RNA reduction level in each period (Fig. 4c).

Drug concentrations and HCV levels in blood correlate with those in the liver

The correlation between telaprevir concentrations in the plasma and liver was analysed in a double logarithmic plot 5 (dose-finding cohort) or 8 h (PK and PK/PD cohorts) after the last dose (Fig. 5). The linear regression lines suggested that telaprevir concentrations in the liver were 5–

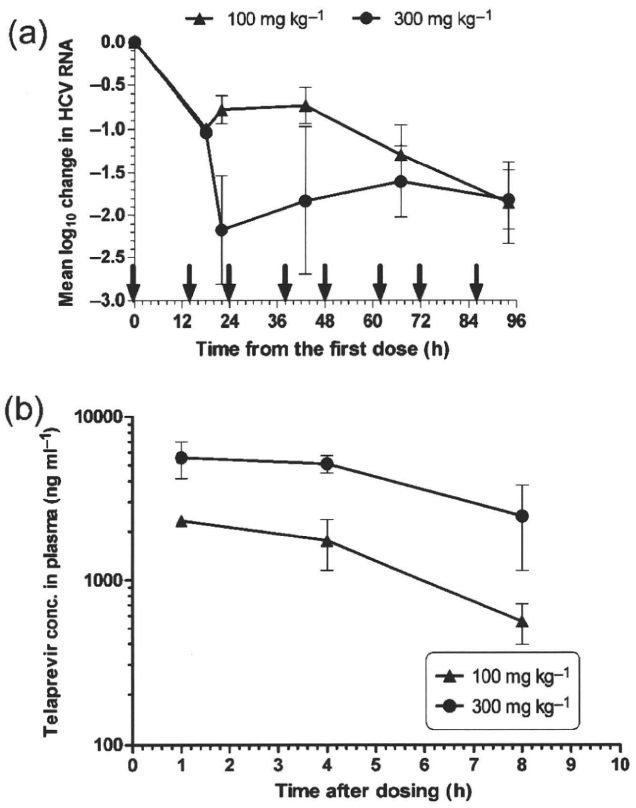

Fig. 3. PK analysis of telaprevir in the HCV-infected mouse model. Six HCV-infected mice were administered 100 (n=3) or 300 (n=3) mg telaprevir kg^{-1} BID for 4 days and serum samples were collected once daily to assess antiviral activity. After the last dose, plasma samples were collected at 1, 4 and 8 h for PK analysis. (a) Mean $\log_{10}$ changes (± SEM) in serum HCV RNA from mice treated with telaprevir. Arrows indicate the times of dosing. (b) Kinetics of telaprevir concentrations in plasma after the last dose.

10-fold higher at 5 h and approximately fourfold higher at 8 h than those in plasma. Total cellular RNA samples were extracted from two, one and four discrete small sections (approx. 50 mg) of the liver in the preliminary dose-finding, PK and PK/PD cohorts, respectively. HCV RNA levels in the total cellular RNA extract were relatively quantified by duplex real-time RT-PCR analysis using human β_2-microglobulin (hβ_2m) as an internal standard of human endogenous gene expression. Neither the threshold cycle (Ct) of hβ_2m ($Ct_{h\beta 2m}$) nor the Ct of HCV (Ct_{HCV}) correlated with total RNA from a small section of the chimeric human livers (data not shown). This result indicated that occupancy rates of human cells varied individually and/or among small sections of the chimeric human liver. Therefore, the mean difference in Ct ($\Delta Ct = Ct_{HCV} - Ct_{h\beta 2m}$) in each mouse was calculated and plotted against the viral load in serum (Fig. 6). After treatment with telaprevir for up to 10 days, mean ΔCt values ranged between 11 (HCV RNA content: $2^{11} = 2 \times 10^3$-fold lower than hβ_2m expression) and 17 (1×10^5-fold lower) among the HCV-infected mice and correlated linearly with $\log_{10}$ serum HCV RNA levels.

Viral dynamics model analysis

To evaluate time-dependent reductions in HCV with BID dosing, 12 HCV-infected elderly mice, which maintained high and steady-state viral loads (1.2×10^6–8.5×10^7 copies ml^{-1}) for more than 6 months, were treated with 200 mg telaprevir kg^{-1} BID for 3 days. The mice were divided into two groups, and serum samples were collected just before the second dose and 4 (n=6) or 8 (n=6) h after every two administrations. The single administration of telaprevir resulted in a mean 0.8–1.0 $\log_{10}$-fold reduction in HCV RNA in both groups. After the second dose, the pattern of viral kinetics appeared to depend on the time of serum collection, and the mean HCV RNA reduction level was higher in the 8 h group than in the 4 h group and plateaued at approximately a 2 $\log_{10}$-fold reduction in both groups after treatment for 3 days (Fig. 7). Finally, we attempted to estimate parameters of efficacy (ε) and virus clearance (c) per hour in this mouse model for comparison with estimates derived from human studies. Because the mean viral kinetics of the 8 h group was biphasic, the values in the 8 h group were used together for the mathematical model analysis. The estimated ε and c values were 0.992 (95 % CI 0.982–1.00) and 0.200 (95 % CI 0.110–0.291), respectively.

DISCUSSION

Using a mouse model with a chimeric human liver for HCV infection, we analysed the PK/PD of telaprevir treatment and investigated HCV dynamics during the initial phase of protease inhibitor treatment. All the mice in this study were expected to have more than half of their livers repopulated by human hepatocytes (Tateno *et al.*, 2004), which simulates a human drug metabolism profile (Katoh *et al.*, 2007, 2008). After the infection with HCV genotype 1b, high viral loads were maintained in the mice for more than 6 months. Recent studies have indicated the utility of a human/mouse chimera model for HCV infection to evaluate antiviral efficacy (Kneteman *et al.*, 2006, 2009) and preclinical safety (Vanwolleghem *et al.*, 2007). However, PK/PD studies and estimations of virus clearance rate have rarely been performed in this mouse model. HCV production, including intracellular replication in engrafted hepatocytes, has also not yet been elucidated. Despite the SCID nature of this mouse model, a 2 $\log_{10}$-fold HCV RNA reduction was observed within 0.5 days, as has been observed previously in CHC patients (Forestier *et al.*, 2007; Reesink *et al.*, 2006). In this mouse model, the rapid rebound in HCV load during the intermission from drug exposure indicated the rapid production and release of HCV into the circulation. This finding indicates that a virion-clearing compartment, which does not depend on T- and B-cell responses, may exist in this mouse model.